

T-4610

**DEHYDROGENATION OF ANTHRAHYDROQUINONES  
OVER SUPPORTED METAL CATALYSTS**

by

**MAZIN YASEEN SHATNAWI**

ProQuest Number: 10796622

All rights reserved

INFORMATION TO ALL USERS

The quality of this reproduction is dependent upon the quality of the copy submitted.

In the unlikely event that the author did not send a complete manuscript and there are missing pages, these will be noted. Also, if material had to be removed, a note will indicate the deletion.



ProQuest 10796622

Published by ProQuest LLC (2019). Copyright of the Dissertation is held by the Author.

All rights reserved.

This work is protected against unauthorized copying under Title 17, United States Code  
Microform Edition © ProQuest LLC.


ProQuest LLC.  
789 East Eisenhower Parkway  
P.O. Box 1346  
Ann Arbor, MI 48106 – 1346

A thesis submitted to the Faculty and the Board of Trustees of the Colorado School of Mines in partial fulfillment of the requirements for the degree of Doctor of Philosophy (Applied Chemistry).

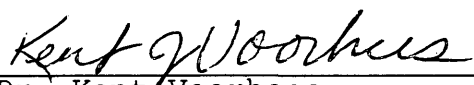
Golden, Colorado

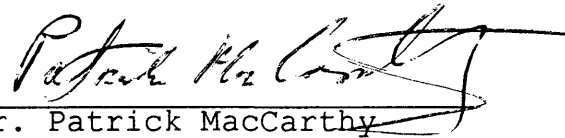
Date 5-31-95

Signed:

  
Mazin Y. Shatnawi


Approved:

  
Dr. Kent Voorhees  
Thesis Advisor

  
Dr. Patrick MacCarthy  
Thesis Co-Advisor

Golden, Colorado

Date 5-31-95

  
Dr. Steven R. Daniel  
Department Head and Professor  
Applied Chemistry

**ABSTRACT**

The efficiency of several catalysts to dehydrogenate 2-t-butyl-9,10-anthrahydroquinone (2-t-butyl-9,10-dihydroxy anthracene) was tested. Commercially available alumina supported chromium oxide and platinum metal catalysts were tested. Several supported platinum, palladium, rhodium, and palladium-gold catalysts were prepared and tested. Lanthanum oxide doped alumina, silica, quartz, and undoped silica were used as catalyst supports. The effect of temperature, pressure, residence time, catalyst particle size, catalyst doping, and catalyst feed additives on the catalyst performance were also investigated. The feed additives used were water, poisoning substances, and coke precursors. A glass reactor was designed and used in the preparation of the catalyst feedstock and a stainless steel catalytic reactor was also designed and used in catalyst testing.

To evaluate the catalysts performance, catalysts were characterized before and after testing and the catalyst feedstock and reaction products were also analyzed. Nuclear

magnetic resonance (NMR) spectroscopy was used as the main technique for the analyses of the liquid reaction products. Two liquid reaction products were also analyzed using gas chromatography-mass (GC/MS) spectrometry. Gas chromatography (GC) was used to analyze the gaseous reaction products. x-Ray diffraction, surface area measurements, and thermal gravimetric analysis were used in catalyst surface characterization and analyses.

Results showed that lanthana doped silica grade 57 was the best catalyst support tested and the use of a more neutral support would enhance the catalyst selectivity. Alumina support was the worst then silica grade 3. Undoped silica and doped quartz came in between. The chromium oxide catalyst was the least hydrogen selective catalyst. Rhodium was the next least then palladium and platinum was the best metal, to be used in catalyst preparation, in terms of hydrogen selectivity.

Hydrogen selectivities of >60% were obtained using a platinum on doped silica grade 57 catalyst. This hydrogen was collected and can be used in industry.

### **Note from the Thesis Committee**

Mr. Shatnawi was hired as a graduate research assistant on a project funded by an oil company to conduct research on petroleum desulfurization catalysis for his Ph.D. degree. Near the completion of the thesis, the company took custody of Mr. Shatnawi's data and refused access thereto. For this reason, the following dissertation was prepared without the availability of the data. Considerable efforts were made to gain access to the data, but all such efforts were in vain. For this reason, the following dissertation was prepared without direct access to the data.

## TABLE OF CONTENTS

ABSTRACT .....	iii
LIST OF FIGURES .....	viii
ACKNOWLEDGMENTS .....	x
DEDICATION .....	xii
INTRODUCTION .....	1
BACKGROUND .....	7
Environmental Requirements .....	7
Conventional Gas Sweetening Processes .....	9
Claus Process .....	10
Stretford™ Process .....	14
Takahax Process .....	18
Chemsweet™ Process .....	20
Lo-Cat™ Process .....	21
Summary .....	23
Direct Hydrogen Sulfide Decomposition .....	24
HYSULF <sup>SM</sup> Process .....	28
Catalytic Hydrogenation of Quinones .....	31
Catalytic Hydrogenation of aldehydes and ketones .....	36
Hydrogenolysis of Aromatic Carbonyls .....	38
Requirements of a Catalyst for HYSULF <sup>SM</sup> Process .....	40
STATEMENT OF THE PROBLEM .....	44
EQUIPMENT AND EXPERIMENTAL PROCEDURES .....	47
Materials Used .....	47

Feedstock and Treatment Chemicals .....	47
Chemicals Used in Catalysts Preparation .....	47
Commercial Catalysts .....	48
Catalysts Prepared by Previous Graduate Students	48
Feedstock Preparation and Glass Reactor Setup .....	49
Catalyst Preparation .....	53
Catalyst Supports .....	53
Untreated Supports .....	53
Treated Supports .....	54
Supported Metal Catalysts .....	55
Lanthana-Doped Catalysts on Silica Grade 3 .....	55
Lanthana-Doped Catalysts on Silica Grade 57	58
Lanthana-Doped Catalysts on Quartz .....	59
Undoped Catalysts .....	60
Electrosputtered Catalyst .....	61
Catalytic Reactor .....	61
Analytical Equipment .....	66
Nuclear Magnetic Resonance .....	66
X-Ray Diffraction .....	67
Gas Chromatography .....	68
Gas Chromatography-Mass Spectrometry .....	69
Thermal Gravimetric Analysis .....	70
Surface Area .....	70
Specific Metal Surface Area (Chemisorption) .....	71
Chloride Analysis .....	72
RESULTS AND DISCUSSION .....	74
General Overview .....	74
Feedstock and Product Analyses .....	78
Results of Analyses Using the 90 MHz	
NMR Instrument .....	81
Results of Analyses Using the 300 MHz	
NMR Instrument .....	86
Results of Gas Chromatographic Analyses .....	88
Results of Gas Chromatography-Mass	
Spectrometric Analyses .....	88

Catalyst Evaluation ..... 89  
    Supported Metal Oxide Catalysts ..... 94  
    Supported Metal Catalysts ..... 94  
        Effect of Support Type on Catalyst Performance 95  
        Effect of Metal Type on Catalyst Performance 103  
        Effect of Metal Concentration on Catalyst  
        Performance ..... 104  
        Effect of Pressure on Catalyst Performance ..... 106  
        Effect of Temperature on Catalyst Performance 107  
        Effect of Residence Time on Catalyst  
        Performance ..... 108  
        Effect of Particle Size on Catalyst Performance 109  
        Effect of Poisons and Coke Precursors on  
        Catalyst Performance ..... 110  
        Effect of Water on Catalyst Performance ..... 112  
Catalyst Hydrogenation Activity ..... 114  
Surface Analyses ..... 115  
    Surface Analyses by X-ray Diffraction ..... 115  
    Thermal Gravimetric Analyses (TG/DTA) ..... 119  
Proposed Dehydrogenation Mechanism ..... 119  
Conclusions ..... 121  
SUGGESTIONS FOR FUTURE WORK ..... 126  
REFERENCES ..... 130

## LIST OF FIGURES

<u>Figure</u>	
1a.	Alkylanthraquinone ring saturation in the autoxidation synthesis of $H_2O_2$ ..... 33
1b.	Other possible side reactions occur in the autoxidation synthesis of $H_2O_2$ ..... 35
2.	Phenol-cyclohexadienone tautomerization ..... 37
3.	The glass reactor used in the preparation of the catalyst feed ..... 50
4.	The stainless steel catalytic reactor ..... 62
5.	Possible quinone derivatives present in the catalytic reaction products mixture ..... 77
6.	A sketch NMR spectra of (A) TBAQ (B) TBAQ and $H_2$ TBAQ in NMP using the 90 MHz NMR instrument ..... 82
7.	A sketch of NMR spectra of (A) typical catalyst feed and (B) catalytic reaction product using the 90 MHz NMR instrument ..... 85
8.	A sketch of signals in the t-butyl region of a (A) catalyst feedstock and (B) dehydrogenation reaction product using the 300 MHz NMR instrument ..... 87
9.	Neutralization of the support acidic sites by the dopant material ..... 97
10.	Production of byproducts in the presence of an acidic catalyst ..... 98
11.	Effect of basic support material on byproducts production in the catalytic dehydrogenation of $H_2$ TBAQ ..... 102

<b>12.</b>	A hypothetical diagram showing the heterogeneity of the catalyst surface .....	113
<b>13.</b>	Possible pathways for reactions occurring during the catalytic reaction .....	120
<b>14.</b>	An illustration of the dehydrogenation reaction on the catalyst surface .....	122

**IN THE NAME OF ALLAH, THE MOST GRACIOUS, MOST MERCIFUL**

**ACKNOWLEDGMENTS**

Praise, glory, and thanks be to Allah the most beneficent, the most merciful, the Cherisher and Sustainer of the Worlds. He who enabled me to successfully complete this project, kept me mentally strong and gave me the courage and peace during the dilemma of my old thesis. Peace be upon his prophet Mohammad and other prophets and messengers who led the people to the right path.

Speaking about the dilemma of my 'old thesis' which I had never been given the chance to defend due to personal interests of the people who were involved directly or indirectly with the project, I would like to thank Professor Patrick MacCarthy, the symbol of humanity, who had been strongly guiding me and helping me out of that dilemma both mentally and physically.

I'd also like to thank Professor Kent Voorhees, the unknown soldier, who had been communicating and fighting to get me out of that sad situation. Words can never be enough to thank these two Professors, Dr. MacCarthy and Dr.

Voorhees. I should also not forget my friends who sympathized with me and tried to help me in any way like Dr. B. Murugaverl (a previous research fellow in Chemistry), and all good Professors and friends of mine.

Speaking about the present situation, I would like to express my gratitude, thanks, and appreciation to Dr. Kent Voorhees, my thesis advisor, and Dr. Patrick MacCarthy, thesis co-advisor, for their continuous assistance, guidance, and intellectual suggestions in making this document possible.

My thanks also go to my thesis Committee members Dr. Robert Baldwin, Dr. George Kennedy, Dr. George Lucas, and Professor Gaby Neunzert, Committee Chairman, for their assistance and sympathy. Thank also go to Ahmad Gharaibeh for his continuous friend ship.

My deepest and greatest gratitude and thanks go to my parents for their efforts in raising me in the nicest way, and providing continuous encouragement and prayers; and to my wife for her patience, encouragement, sacrifice, and suffering. Finally, my thanks also go to the Jordan University of Science and Technology for the scholarship with which I came to pursue my Ph.D. degree.

T-4610

DEDICATION

TO MY PARENTS, WIFE, SON,  
BROTHERS, AND SISTERS

## CHAPTER 1

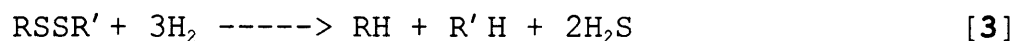
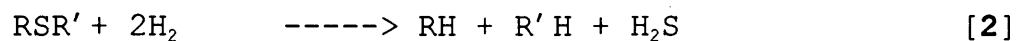
### INTRODUCTION

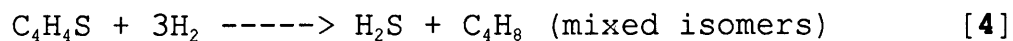
The presence of sulfur-containing compounds accompanied with hydrocarbon fossil fuels such as natural gas, crude oil, coal, and oil shale is attributed to the biological origin of these fuels. Due to the diversity in biomass composition from which these fuels were derived, the amount and type of sulfur compounds present in hydrocarbon fuels varies in the range of 0.05 to 14 weight percent (1,2).

Mercaptans, sulfides, disulfides, and thiophenes are the typical sulfur-containing compounds present in petroleum and heavier fossil fuels. The majority of the commercially processed crude oils contain no more than 4 weight percent of these organosulfur compounds. In natural gases, the amount of sulfur-containing compounds present varies from negligible to over 90 mole percent. While hydrogen sulfide is the main sulfur compound in low-sulfur natural gases, high-sulfur gases contain entrained elemental sulfur.

Due to the fact that simple mercaptans, sulfides, and disulfides are thermally less stable than their higher molecular weight analogues or thiophenes, they often decompose during distillation to produce hydrogen sulfide. Generally, these sulfur compounds produce hydrogen sulfide during the distillation, hydrotreating and cracking steps in the refining processes (2,3,4).

Sulfur levels in distillate fractions to be sent to naphtha reforming or catalytic cracking units must be significantly reduced to prevent catalyst poisoning. These distillates are typically hydrotreated over a sulfided cobalt-molybdenum or nickel-tungsten catalyst at 350-450°C and 500-1000 psig of hydrogen. Catalytic hydrotreatment of distillates involves many chemical transformations including hydrogenation, hydrocracking, and hydrodesulfurization. Equations [1] through [4] show the production of lower molecular weight hydrocarbons and hydrogen sulfide from thiols, sulfides, disulfides, and thiophenes during the hydrodesulfurization process.





Unfortunately, the demand for hydrogen, required during the hydrotreating process in a refinery always exceeds the available hydrogen generated from other processes like reforming.

Catalytic hydrocracking of heavy oil distillates converts the high molecular weight sulfur compounds to hydrogen sulfide, and/or lower molecular weight sulfur compounds, and hydrocarbons. These lower molecular weight sulfur compounds can further produce hydrogen sulfide. Studies have shown that mercaptans and sulfides evolve hydrogen sulfide more readily than thiophenes (3). It is obvious that, in a refinery, the production of refined fuel products is accompanied by the production of hydrogen sulfide.

Since hydrogen sulfide is toxic, air pollution regulations require that most of it be removed from natural and refinery fuel gases and converted into environmentally safe products such as elemental sulfur and water (3,5,6). Upon combustion, hydrogen sulfide and organic sulfur compounds produce sulfur oxides ( $\text{SO}_x$ ). Medical studies have

shown that contact with sulfur oxides has adverse health effects on humans and other animals. Therefore, sulfur oxides are Federally regulated pollutants (7). Furthermore, sulfur oxides can combine with atmospheric moisture to form sulfuric acid, a vital component of acid rain. However, besides the pollution issues, these sulfur compounds have very unpleasant odors that makes handling fuel liquids very undesirable.

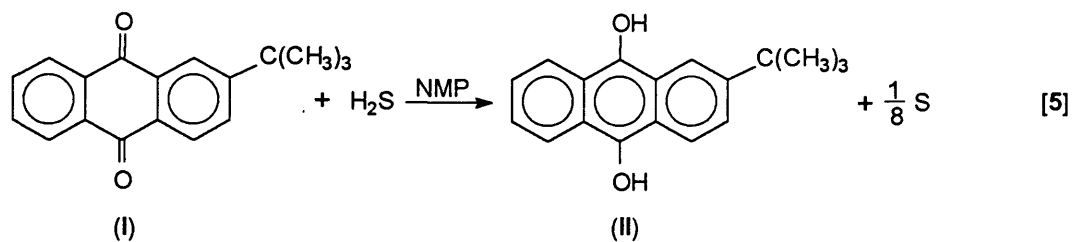
Unfortunately, in all the commercially used sour gas treatment processes such as Claus, Stretford<sup>TM1</sup> and Takahax processes hydrogen sulfide is converted into sulfur and water rather than hydrogen, a potentially valuable element in refining (8,9). Until recently, the only available means for converting hydrogen sulfide into sulfur and hydrogen were high temperature thermal decomposition processes (10,11,12). The high temperature requirement of these processes results in a high cost for commercial use. A low temperature process for the transformation of hydrogen sulfide into hydrogen and sulfur has only recently been reported (13). The new process, called HYSULF<sup>SM2</sup> (14), can

---

<sup>1</sup> TM = Trade Mark of Clayton Aniline Company and North Western Gas Board.

<sup>2</sup> SM = Service Mark of Marathon Oil Company.

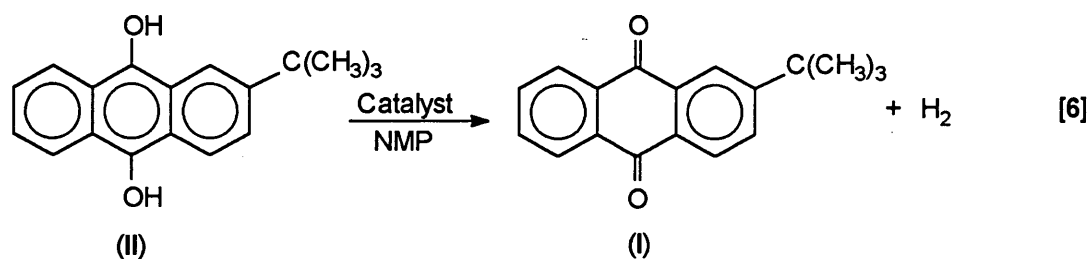
potentially overcome many of the disadvantages associated with existing sour gas treatment methods (for more discussion see References 13 and 14). The HYSULF<sup>SM</sup> process consists of two stages, a sulfur production stage and a hydrogen generation stage. In the first stage, studied by Krisanti (14), hydrogen sulfide is absorbed into a nonaqueous solution containing a quinone compound. Hydrogen sulfide is used as a reducing agent to convert the quinone, 2-t-butyl-9,10-anthraquinone (TBAQ, **I**); into a hydroquinone, 2-t-butyl-9,10-dihydroxyanthracene (H<sub>2</sub>TBAQ, **II**); Equation [5]. Elemental sulfur forms during the reduction process, precipitates from the solution and is removed by filtration.



NMP = N - Methyl - 2 - pyrrolidinone

In the second stage the hydroquinone (**II**) product is catalytically converted to the original quinone (**I**) and

hydrogen, Equation [6].



Although this process looks very promising, very little is known about its fundamental chemistry and reaction kinetics. This information is important for further development and commercialization. Since the first stage had been studied (14), the focus of this study is to better understand the second stage and develop a catalyst to achieve optimum activity and selectivity for the conversion of the hydroquinone into quinone and hydrogen.

## CHAPTER 2

### BACKGROUND

Due to their environmental impact, the chemistry of sulfur-containing compounds associated with crude oils has attracted the attention of both fuel industries and the environmental regulatory agencies. The efforts have been focused on understanding the fundamental chemistry and behavior of these compounds accompanied with developing new processes for their removal from petroleum and natural gas products.

#### 2.1 ENVIRONMENTAL REQUIREMENTS

In 1973, petroleum refining became one of the first industries to be regulated by Environmental Protection Agency (EPA) in the United States (15). Emissions of gaseous pollutants such as nitrogen oxides ( $\text{NO}_x$ ), sulfur oxides ( $\text{SO}_x$ ), carbon monoxide (CO), particulates, and hydrocarbons (HC) are of most concern.

Sulfur oxides  $\text{SO}_2$  and  $\text{SO}_3$  are produced from the combustion of sulfur-containing compounds such as

mercaptans, thiophenes, and sulfides. These two oxides are commonly referred to as  $\text{SO}_x$ . Sulfur trioxide ( $\text{SO}_3$ ) is highly toxic to humans, an irritant, and strongly corrosive to mucous membranes (16). Upon contact with moisture, this emitted trioxide is rapidly converted into sulfuric acid ( $\text{H}_2\text{SO}_4$ ) in the atmosphere. This sulfuric acid dissolves in water droplets or adsorbs onto dust particulates and falls as acid-rain or dry deposits. The pH of rainfall in the United States of America can range between 4.2 in the northeastern part to 5.0 in the western part. Approximately, 65% of the pH decrease is attributed to sulfur oxides and 35% to nitrogen oxides ( $\text{NO}_x$ ) emissions (7).

Sulfur dioxide ( $\text{SO}_2$ ), a colorless gas with a strong suffocating odor and intensely irritating to the eyes and respiratory tract is the primary  $\text{SO}_x$  pollutant in the United States (16). While in the atmosphere,  $\text{SO}_2$  is converted to  $\text{SO}_3$  by direct oxidation. However, this direct oxidation is slow and its contribution to the disappearance of  $\text{SO}_2$  is insignificant compared to other chemical processes (7).

According to the Clean Air Act of 1970,  $\text{SO}_x$  emissions should be within predetermined pollution limits established

by the EPA (17). The sulfur content of a crude oil can be used to indicate the expected  $\text{SO}_x$  emissions from that fuel source (7). In order to sell a gas, the gas producer must meet specific standards. Such standards include a maximum  $\text{H}_2\text{S}$  content of  $5.72 \text{ mg/m}^3$ , a maximum mercaptan content of  $22.91 \text{ mg/m}^3$ , and a maximum water content of  $64\text{-}112 \text{ mg/m}^3$ . To comply with these standards and avoid the penalty of violation, fuel producers have developed treatment facilities to remove the potentially hazardous sulfur compounds. In these refinery facilities, organosulfur compounds are converted to hydrogen sulfide and hydrocarbons. The hydrogen sulfide is subsequently converted into environmentally safe products (8).

## **2.2 Conventional Gas Sweetening Processes**

The majority of the gas sweetening (sulfur removal) processes available have been developed to be used by the refining and natural gas industries. In selecting a certain gas sweetening process, one should consider the following aspects (18).

1. The type and amount of impurities needed to be removed prior to treatment.
2. The initial impurity concentration and degree of removal required.
3. The volume of gas to be treated.

4. The pressure and temperature of the sulfur-containing gas stream to be processed.
5. The nature of the final sulfur products.

These factors along with other considerations are used in determining which process is best suited for a given sulfur-containing gas. The most popular of the many gas sweetening processes available are the Claus, Stretford<sup>TM</sup>, Takahax, Chemsweet<sup>TM3</sup>, and Lo-Cat<sup>TM4</sup>. Therefore, it is of importance to discuss these processes along with their advantages and disadvantages and compare them with the new potential processes (the direct hydrogen sulfide decomposition and the HYSULF<sup>SM</sup>).

### 2.2.1 Claus Process

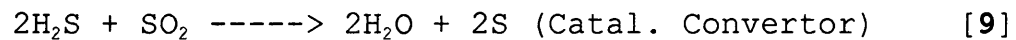
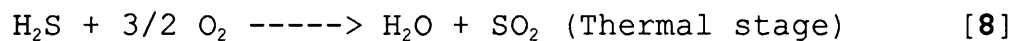
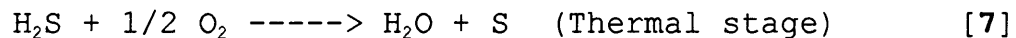
This process was invented in 1883 and has been used on a large scale in the United States of America since the 1950's (8,9). It was originally designed for the recovery of sulfur from pure hydrogen sulfide or acid gas streams containing high concentrations of hydrogen sulfide. Acid gas streams are those streams of gas stripped from regenerable alkaline solutions or physical solvents used in

---

<sup>3</sup> TM-Chemsweet = Trade Mark of C-E Natco Company.

<sup>4</sup> TM-Lo-Cat = Trade Mark of ARI Technologies, Inc.

the purification of sour gases. The process consists of two main stages, the thermal stage and the catalytic convertor stage. Since its invention, the process has undergone several modifications. The principal chemical reactions of the process are presented in equations [7] through [9].



In the thermal stage, the reaction furnace must be held at a temperature above 538°C (1000°F). The catalytic convertor temperature has to be maintained between 371°C (700°F) and somewhat above 280°C (536°F), the sulfur dew-point. The catalyst used in this process is natural bauxite (Al<sub>2</sub>O<sub>3</sub>.2H<sub>2</sub>O) or alumina (Al<sub>2</sub>O<sub>3</sub>) shaped into pellets or balls. Due to its higher activity and attrition resistance, alumina is preferred over bauxite in high efficiency plants. Two approaches can be used in operating a Claus plant. The first approach (the partial combustion process) is used for acid-gas streams that exceeds 50% of hydrogen sulfide on a volume basis. In this process, the entire acid-gas stream is combined with a carefully controlled amount of air sufficient to convert one third of the H<sub>2</sub>S into SO<sub>2</sub>.

Substantial amounts of gaseous elemental sulfur are formed at the preferred temperature range of the furnace, typically 1093-1649°C (2000-3000°F). This sulfur is subsequently removed in a cooled condenser adjacent to the furnace. The acid-gases leaving the sulfur condenser are then reheated and fed to the catalytic convertor. If the gas feed temperature is not above the dew-point of sulfur, as it passes through the catalytic convertor, rapid catalyst deactivation occurs due to poisoning by sulfur.

Additional sulfur is produced from the reaction of hydrogen sulfide with sulfur dioxide in the catalytic convertor (Equation [9]) and should be removed using a second cooled condenser. Effluent gases are treated in the same manner using successive catalytic convertors, condensers, and reheating the effluent after each cooler until the exhaust gases meet acceptable sulfur emission standards.

The second approach (the split stream process) is used for acid-gas streams of low hydrogen sulfide concentration. One third of the acid-gas is split from the main gas stream and mixed with a stoichiometric amount of air. The reaction mixture is then fed to a furnace where the hydrogen sulfide

is combusted to sulfur dioxide. The hot emerging sulfur dioxide is then cooled, recombined with the main gas stream, and introduced to the first catalytic reactor. The rest of the operation is identical to the "partial conversion process".

As with any other industrial facility, the Claus process has some advantages such as its use in large scale, high hydrogen sulfide content gas treatment plants, and the production of extremely high quality sulfur. On the other hand, the process has some disadvantages such as:

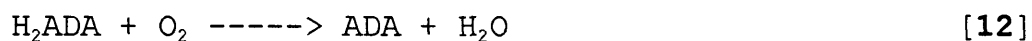
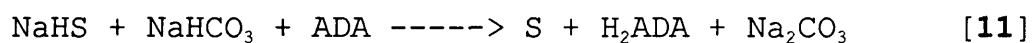
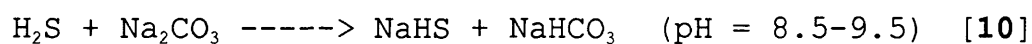
- The need for two or more catalytic convertors in order to achieve low  $\text{SO}_2$  and  $\text{H}_2\text{S}$  emissions;
- The installation of mist eliminators after each sulfur condenser to avoid catalyst deactivation through poisoning;
- The complete conversion of  $\text{H}_2\text{S}$  to elemental sulfur is impossible due to equilibrium limitations of the reaction. As a result,  $\text{SO}_x$  and  $\text{H}_2\text{S}$  emissions exceed the prescribed levels, hence, many Claus units are required;
- The precise control of air to acid-gas ratio is difficult;
- The molar ratio of  $\text{H}_2\text{S}$  to  $\text{SO}_2$  in the reaction gas stream entering the catalytic convertor should be maintained at 2:1 ( $\text{H}_2\text{S}:\text{SO}_2$ ) in order to achieve maximum conversion. Any deviation in this ratio results in an unacceptable emission;

- The precise control of temperature is necessary to prevent sulfur from plugging the equipment;
- The reaction furnace temperature must be sufficiently high to oxidize all hydrocarbons to  $\text{CO}_2$  and  $\text{H}_2\text{O}$  to avoid catalyst deactivation by carbonaceous deposit;
- The presence of water and sulfur often causes a common plugging problem which can force the shutdown of the unit;
- The production of water in conjunction with the presence of hydrogen sulfide, and sulfur dioxide leads to severe corrosion of the refinery equipment;
- The use of three to four catalytic convertors increases the net operational cost; and finally,
- The hydrogen present in  $\text{H}_2\text{S}$  is converted to water.

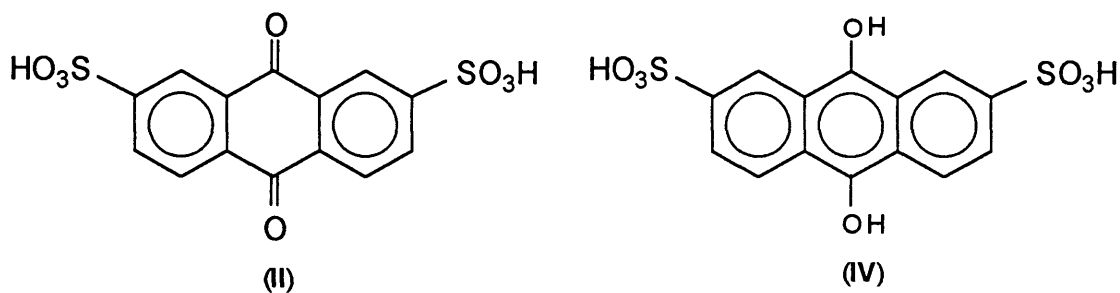
### **2.2.2 Stretford™ Process**

This process was developed in the United Kingdom by the Clayton Aniline Company and the North Western Gas Board (8,9). It was initially designed for the removal of hydrogen sulfide from coal gas. Later, it was used for the desulfurization of refinery tail gas, synthesis gas, natural gas, and other hydrocarbon liquids. The original process involved the utilization of an aqueous solution of sodium carbonate ( $\text{Na}_2\text{CO}_3$ ) and bicarbonate ( $\text{NaHCO}_3$ ) in a 1:3 mole ratio, which results in a pH of 8.5 to 9.5, and sodium salts

of the 2,6- or 2,7-isomers of 9,10-anthraquinone disulfonic acid. The easy regeneration of the working solution and the low cost of the equipment made this process a viable alternative to the Claus process. The overall chemical transformations involved are presented in Equations [10] through [12].



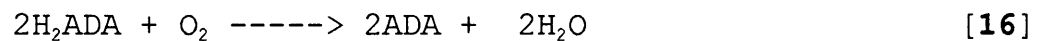
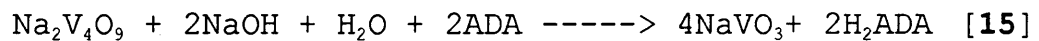
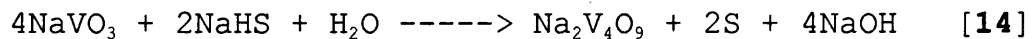
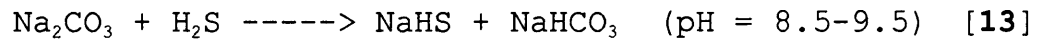
(where ADA = 9,10-anthraquinone-2,7-disulfonic acid (III);  
H<sub>2</sub>ADA = 9,10-dihydroxyanthracene-2,7-disulfonic acid (IV)).



The presence of dissolved oxygen with the absorbed hydrogen sulfide, at >40 ppm loadings of H<sub>2</sub>S, in the aqueous sodium

carbonate solution (Equation [10]) causes a side reaction to occur through which sodium thiosulfate is formed.

Therefore, hydrogen sulfide loading is limited to 40 ppm in order to prevent this side reaction. This problem is largely eliminated by the addition of a sodium metavanadate ( $\text{NaVO}_3$ ) catalyst to the solution. The catalyst increases the rate of sulfur formation at the expense of thiosulfate production. Consequently, it is possible to increase the hydrogen sulfide loadings to 500-1000 ppm range. Equations [13] through [16] describe the modified version of the process.



From the above equations, it is clear that for each mole of  $\text{H}_2\text{S}$  consumed two moles of metavanadate are required. In practice, excess catalyst is added to avoid the formation of thiocyanate during the regeneration step (Equation [16]). Although the regeneration step is relatively rapid, it can be accelerated by the addition of a small amount of iron-EDTA. When the amount of absorbed hydrogen sulfide exceeds

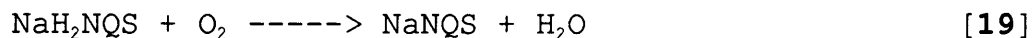
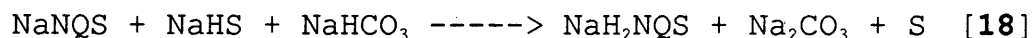
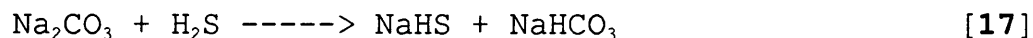
the vanadate catalyst capacity, a black insoluble vanadium-oxygen-sulfur complex is formed. The use of a continuous air purge over a long period of time restores the soluble form of the catalyst. Formation of the insoluble complex can be prevented by the addition of sodium tartrate.

In its application the Stretford process encounters several disadvantages such as:

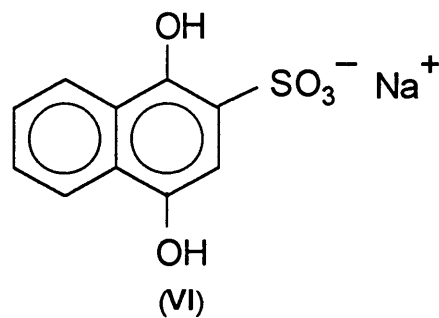
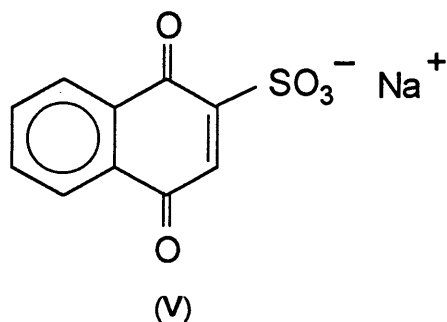
- The restricted  $H_2S$  limits its conversion so larger liquid recirculation rates and power consumption, are necessary to compensate for the lower reaction rate;
- The difficulty in handling the caustic aqueous sulfur systems and the undesirable corrosion they cause to equipment;
- The formation of hazardous byproducts, thiocyanate, adds an additional environmental waste problem;
- The clogging of refinery equipment;
- The contamination of the aqueous systems by bacteria which may grow into large masses that interfere with the process;
- Finally, the valuable hydrogen in hydrogen sulfide is lost as water.

### 2.2.3 Takahax Process

The Takahax process was developed in Japan by the Tokyo Gas Company and is similar to the Stretford process. It was commercially applied in 1962 to desulfurize coal gas and has been used in over 60 Japanese plants (8,18). The process operates on a cyclic basis and requires no heat. In this process,  $H_2S$  is absorbed by an aqueous solution of sodium carbonate and sodium-1,4-naphthoquinone-2-sulfonate (V) ( $NaNQS$ ). The principal chemical reactions are presented in equations [17] through [19],



(where  $NaH_2NQS$  = sodium-1,4-dihydroxynaphthalene-2-sulfonate (VI)).



The process is well suited for the treatment of refinery tail gases, coke-oven gases, and waste gas streams. From Equations [17] through [19], it is obvious that the process involves the reversible redox properties of the quinone-hydroquinone system.

The Takahax process has some advantages over the more conventional processes. These are:

- The cost of the oxidation step is significantly reduced by eliminating the expensive and troublesome catalyst;
- The specific control of the air-to-gas ratio is not needed;
- No heating is required;
- Carbon dioxide is easily removed from the aqueous system by stripping it with air;
- Sulfur dioxide, sulfur trioxide, and hydrogen cyanide are absorbed by the aqueous media and converted into sodium sulfate or thiocyanate; And finally,
- Simple equipment design is used.

On the other hand, the Takahax process has some disadvantages such as the accumulation of sodium sulfate and thiocyanate where a bleed stream is needed to keep them at an acceptable level. This accumulation creates a chemical

waste disposal problem. Moreover, as with other processes, hydrogen is lost through its conversion to water.

All of the processes discussed so far are commonly used for large scale operations. The high cost of these processes makes them less favored for small scale operations. The following processes have the flexibility to be used in both large and small scale applications.

#### **2.2.4 Chemsweet™ Process**

The Chemsweet™ process was developed by C-E Natco as an alternative process to the iron sponge and amine processes (20). In 1979, over twenty units were operating in the United States. In this process, the sour gas stream is saturated with water vapor in order to absorb hydrogen sulfide. The wet gas is then bubbled through a water slurry containing inorganic zinc compounds and a dispersant to keep the solid particles in suspension. Zinc ions react instantaneously with sulfide and bisulfide ions, formed upon the absorption of  $H_2S$  in the aqueous media, to form zinc sulfide. This sulfide is then dumped into landfills.

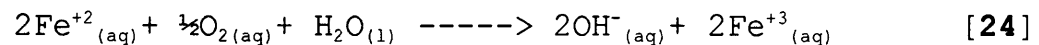
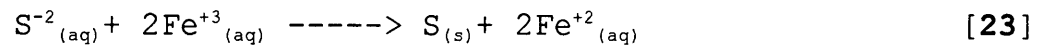
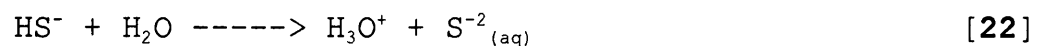
The process has several advantages such as being simpler than the iron sponge-amine process, constant

supervision is not needed, the equipment is easy to service, and a rapid and complete removal of hydrogen sulfide is obtained. However, the process is still accompanied by several problems like the use of aqueous media in connection with  $H_2S$  and  $SO_2$  that result in equipment corrosion, sulfur precipitation as a fine powder which makes its separation difficult and time consuming. Also, the inlet gas must be saturated with water vapor to avoid drying of the slurry and its entrainment by the gas. The inlet gas must be free of liquid hydrocarbons that may coat the solids in the slurry, and thus reduce their catalytic efficiency to convert  $H_2S$  and increase the tendency of the slurry to foam. The slurry contains residual  $H_2S$ , has to be replaced every 15-90 days, and if dumped in landfills, produces an environmental problem. Furthermore, preventive methods are required to keep the slurry from freezing in cold weather. This becomes an important issue for regions with cold climates such as Alaska, Siberia, Colorado, parts of Canada, and northern Europe. Finally, the hydrogen present in  $H_2S$  is converted to water.

#### **2.2.5 Lo-Cat™ Process**

This process was developed by ARI Technologies, Inc. (21,22). It directly converts hydrogen sulfide, in gas

streams, into water and sulfur. It was reported to be a very efficient process with efficiencies up to 99.99%. The basic chemical reactions of this process are summarized in equations [20] through [24].



The catalyst consists of a dilute aqueous solution of a polyhydroxylated sugar and EDTA-chelated iron. The process takes advantage of the redox chemistry of ferric and ferrous ions. Ferric ions are reduced to ferrous ions by hydrogen sulfide to produce  $\text{H}^+$  and elemental sulfur (see Equations [20] to [23]). Instead of forming iron sulfide, as in the iron sponge process, iron ions remain in solution. The fine solid sulfur is circulated until the particle size becomes large enough to precipitate, and then is separated. To regenerate the catalyst, the working solution is contacted with air at a pH of 8.0-8.5 (Equation [24]). It was reported that the process has extremely high catalyst activity, complete nontoxicity of the catalyst solution,

great flexibility of application, insensitivity to gas composition, low cost, and low temperature requirements (5-50°C) (21,22).

However, this process suffers from some disadvantages like the formation of the thiosulfate, a non desirable chemical waste. Sulfur particles have to be circulated until the particle size is large enough to settle down on the bottom of the absorber-oxidizer vessel. The use of aqueous media creates a problem with sulfur recovery and causes corrosion of the refinery components. A significant portion of the iron catalyst is lost through the formation of undesired side products and must be replaced. Finally, the valuable hydrogen in hydrogen sulfide is lost as water.

#### **2.2.6 Summary**

Recently, due to the high demand on gasoline fluids, the removal of hydrogen sulfide from natural gas and refinery tail gases became a very important process. Billions of cubic meters of hydrogen sulfide are annually converted to sulfur and water (23). In summary, several critical difficulties are associated with the existing sour gas treatment processes. The major problems are; 1) the loss of valuable hydrogen as water; 2) the difficulty of

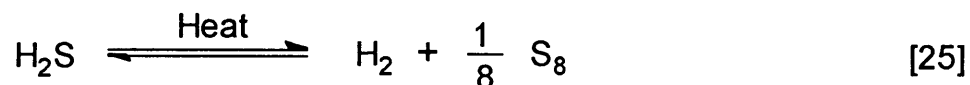
sulfur recovery and equipment corrosion in aqueous systems; 3) the high temperature requirement, and 4) the SO<sub>x</sub> emissions associated with dry systems.

Processes mentioned thus far are examples of the present day acid gas treatment techniques. It is clear that many problems have yet to be solved. The direct hydrogen sulfide decomposition process represents a potentially new technology aimed at addressing some of these problems, especially the loss of the valuable hydrogen as water.

### **2.3 Direct Hydrogen Sulfide Decomposition**

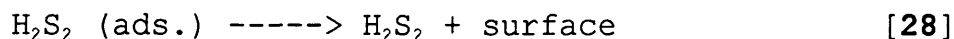
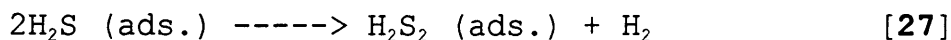
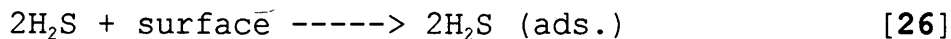
Although it is a fairly stable sulfide, hydrogen sulfide can be thermally decomposed to hydrogen and sulfur. Since the reaction is endothermic, it is thermodynamically unfavorable at temperature below 1527°C (1800°K). The variation of hydrogen yield with temperature, residence time, the effect of physically active catalysts or chemically active metal catalysts on the decomposition reaction have been studied (10). It has been found that above 977°C (1250°K), the reaction proceeds without a catalyst and yields are almost identical to those predicted on simple equilibrium thermodynamic grounds. Below 977°C the reaction rate becomes sufficiently slow to the point

where the equilibrium levels of hydrogen are not reached. At this point, below 977°C, the effect of catalysts becomes increasingly marked. This behavior can be explained on the basis of the reaction mechanism. The presence of chemically active catalysts such as platinum and palladium resulted in greater yields of hydrogen compared to the physically active ones, like molecular sieves.



Since the decomposition reaction is equilibrium controlled continuous removal of one of the products, such as hydrogen, is necessary to drive the equilibrium further to the right, hence, the use of platinum or palladium membranes was suggested. A two step reaction mechanism, for the metal catalyzed reaction, has been proposed, Equations [26] to [29].

Step 1:



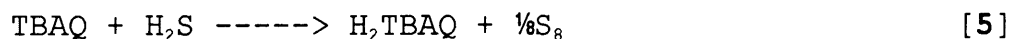
Fukuda *et al.* reported on the catalytic decomposition of  $H_2S$  using molybdenum sulfide and tungsten sulfide catalysts (11). They found that, in the temperature range of 550-750°C, the use of catalyst drastically increased the decomposition rate of  $H_2S$  compared to the uncatalyzed tests. The authors reported that the effect of the catalyst on the decomposition rate decreased with the increase in temperature beyond 550°C. Ratios of the initial decomposition rates (mol%/min) of the catalyzed vs the uncatalyzed tests were reported. At 550°C the initial decomposition rate of the catalyzed test was 50 times greater than that of the uncatalyzed test. At temperatures of 700°C, 750°C, and 800°C the ratios of the initial rates of the catalyzed to the uncatalyzed tests were 34, 24, and 8, respectively (11).

In 1980, Chivers and coworkers reported the use of metal sulfided catalysts for the decomposition of hydrogen sulfide into hydrogen and sulfur in a tubular flow system at 400-800°C. Different sulfides of chromium, molybdenum, tungsten, iron, cobalt, nickel, and copper were tested. They found that below 600°C  $Cr_2S_3$  and  $WS_2$  gave higher hydrogen yields than  $MoS_2$ , while above 600°C the  $MoS_2$  catalyst gave better activity. At temperatures above 800°C,

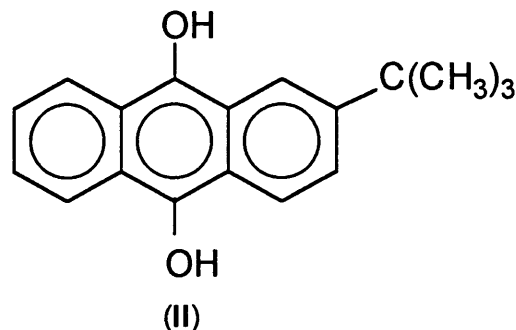
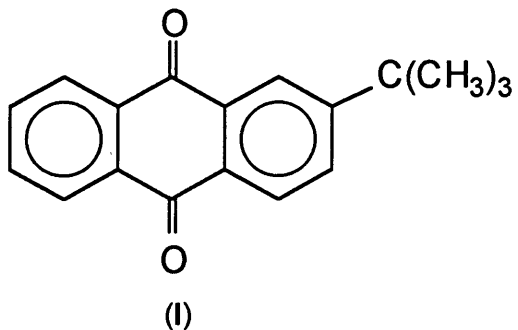
MoS<sub>2</sub> gave higher hydrogen yields (8.5%) compared to the uncatalyzed thermal decomposition test (6.0%) under the same conditions. This means that MoS<sub>2</sub> is functioning as a decomposition catalyst. However, the tested Cr<sub>2</sub>S<sub>3</sub> catalyst showed a small weight loss during the test indicating some catalyst decomposition. MoS<sub>2</sub> and WS<sub>2</sub> showed no weight loss symbolizing more stable catalysts for the decomposition of H<sub>2</sub>S compared to Cr<sub>2</sub>S<sub>3</sub>. They also reported that below 550°C, FeS<sub>2</sub>, CoS<sub>2</sub>, and NiS<sub>2</sub> showed some catalytic activity but started to decompose above this temperature resulting in a corresponding decrease in activity. On the other hand, testing the monosulfides FeS, CoS, and NiS below 400°C gave relatively high initial hydrogen yields compared to other sulfides but the catalyst activity eventually reached a lower steady state value. The authors have attributed this behavior of the monosulfides to their further sulfidation to higher sulfides by H<sub>2</sub>S (12). It is worth mentioning that this study was a fundamental laboratory study and if a hydrogen sulfide treatment process is to be developed, a more thorough understanding of the reactions involved has to be achieved. The low activity of the catalysts indicates that the process is not promising to be used commercially. At the same time, the high temperature requirement and loss of catalyst materials are disadvantages of the method.

## 2.4 HYSULF<sup>SM</sup> Process

This process takes advantage of the redox properties of quinone-hydroquinone systems. Hydrogen sulfide is converted into sulfur and hydrogen in a two stage method. The reactions involved are presented in Equations [5] and [6].



In the first stage, hydrogen sulfide is used to reduce 2-t-butyl-9,10-anthraquinone (TBAQ, **I**) to 2-t-butyl-9,10-dihydroxyanthracene (H<sub>2</sub>TBAQ, **II**). Elemental sulfur is produced during this reduction step. This step is conducted in a non-aqueous solvent under mild reaction temperatures and pressures. In the second stage, H<sub>2</sub>TBAQ is catalytically oxidized (dehydrogenated) to the original TBAQ and molecular



hydrogen is formed. The hydrogen gas produced is now available for other chemical applications. The net result of this process is the conversion of hydrogen sulfide into an environmentally acceptable form of sulfur and hydrogen gas.

Conceptually, the HYSULF<sup>SM</sup> process has the following advantages over the existing commercially used technologies. First, the overall reaction chemistry is greatly simplified relative to existing technologies. Second, the use of the non-aqueous media makes sulfur recovery easier, reduces metal corrosion, and eliminates bacterial growth problems. In fact, no water is produced, and hence, problems associated with its presence are eliminated. Third, hydrogen sulfide is mostly removed as elemental sulfur, thus, eliminating SO<sub>x</sub> gases production and the need for additional tail gas treatment facilities. Fourth, the overall cost of the process is reduced due to the mild reaction conditions used. Fifth, the efficiency of hydrogen sulfide absorption from the acid gas stream and its conversion to sulfur and hydrogen substantially reduces the size of the operation. Sixth, perhaps most important, the valuable hydrogen in hydrogen sulfide is recovered and utilized for further use.

Although this process has tremendous potential, its fundamental chemistry is very complex and not fully understood. Knowledge of the reaction chemistry and kinetics is critical for further development of this technology. A fundamental study of the first stage was done by Krisanti and will not be discussed in further detail here (14). There is a critical need to understand the catalytic stage, and to design, test, and modify candidate catalysts to achieve the best activity and selectivity towards the production of hydrogen. The understanding and investigation of the basic catalytic process involved in the second stage is the subject of this study.

Unfortunately, a thorough literature search reveals a lack of information on direct catalytic dehydrogenation of hydroquinones to quinones and hydrogen. This paucity of literature led to the search for catalytic dehydrogenation of species similar to hydroquinones in their chemical structures.

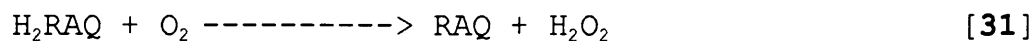
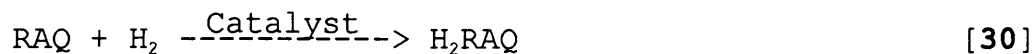
There is a large volume of literature, mostly in the form of patents, that describes the catalytic hydrogenation of quinones to hydroquinones. Quinone hydrogenation is the first step in a two-step process used industrially for the

production of hydrogen peroxide (24). The principle of "microscopic reversibility" suggests that catalysts which are good for the hydrogenation of quinones to hydroquinones will also be good for the reverse process. Therefore, the literature on this topic is included here.

Even there is a big differences in chemical behavior between aromatic alcohols (phenols) and hydroquinones, in essence, quinones can be structurally classified as aromatic alcohols. The dehydrogenation of alcohols into ketones or aldehydes is well known. By the same token, catalysts that have been successfully used for the dehydrogenation of alcohols may also be good candidates for the dehydrogenation of hydroquinones.

## 2.5 Catalytic Hydrogenation of Quinones

Hydrogen peroxide is commercially prepared using the anthraquinone autoxidation method (24,25,26,27). The chemistry of this process is represented in Equations [30] and [31].



(where RAQ = alkylanthraquinone (VII); H<sub>2</sub>RAQ = alkylanthrahydroquinone (VIII)).

In the first step RAQ is catalytically hydrogenated to H<sub>2</sub>RAQ. The peroxide is then generated by purging the reaction mixture with air (Equation [31]) which oxidizes H<sub>2</sub>RAQ back to RAQ.

According to the principle of "microscopic reversibility", a catalyst that has a hydrogenation activity toward a certain group of compounds will, presumably, be able to do the reverse process, i.e. dehydrogenation. Therefore, Equation [30] is of special interest to this study where the reduction of RAQ is typically carried out at temperatures in the 40-50°C range and hydrogen pressures of 4 atmospheres (58.8 psig). Unfortunately, the hydrogenation of RAQ is subject to a number of side reactions (28). These possible side reactions are presented in the schemes shown in Figures **1a** and **1b**. If the reaction conditions are severe enough, the aromatic rings of the H<sub>2</sub>RAQ (**VIII**) can be hydrogenated (saturated) to yield the 5,6,7,8-tetrahydroanthrahydroquinone (**IX**) and the 1,2,3,4,5,6,7,8-octahydroanthrahydroquinone (**X**), see Figure **1a**. The H<sub>2</sub>RAQ (**VIII**) can also undergo tautomerization to form the hydroxyanthrones (oxanthrones) (**XI**) and (**XII**). Catalytic hydrogenolysis (cleavage) of the hydroxyanthrone C-O bond in the hydroxyl

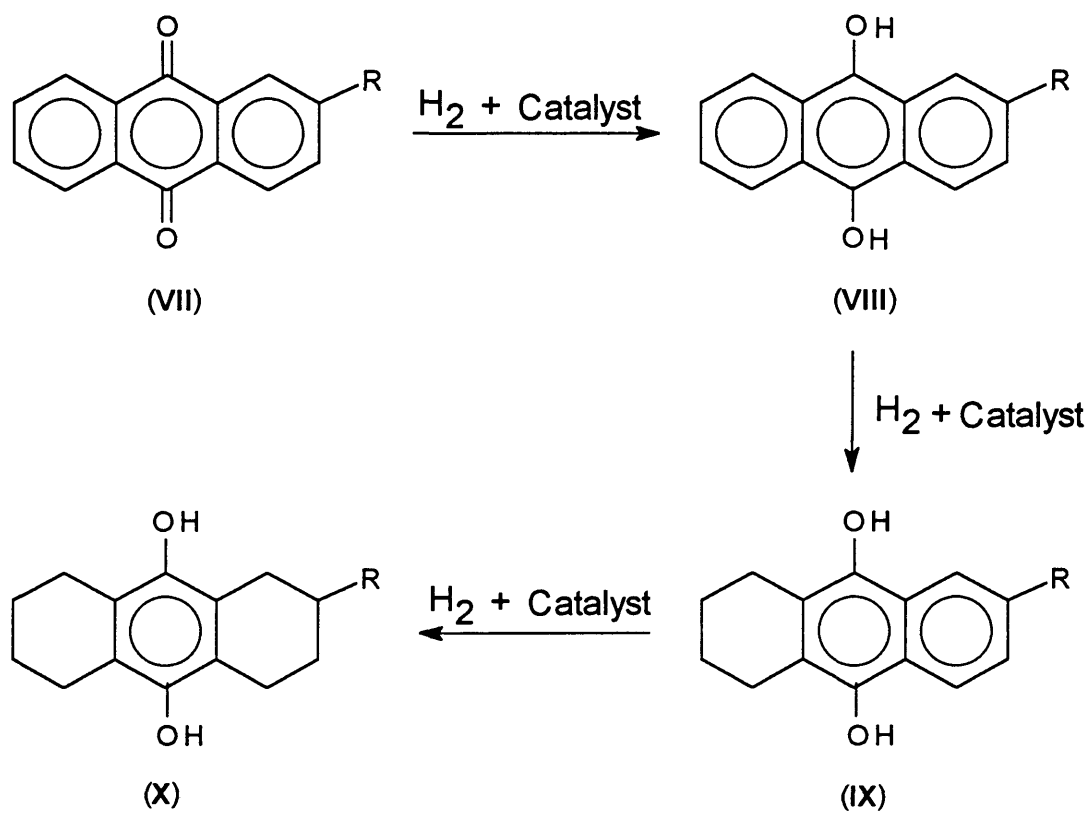


Figure 1a: Alkyanthraquinone ring saturation in the autoxidation synthesis of H<sub>2</sub>O<sub>2</sub>.

group produces the anthrones (**XIII**) and (**XIV**), see Figure **1b**. The concentration of these side products increases with each process cycle and gradually diminishes the efficiency of the process. For this reason, the RAQ conversion level is limited to approximately 50% conversion to minimize the formation of these undesirable side products.

Typically, the catalysts used in this process are Ni, Pd, or Pt metals supported on a high surface area alumina or carbon. The metal function of the catalysts exhibits both hydrogenation and hydrogenolysis activity (29,30,31). The hydrogenation function is desirable to convert RAQ to H<sub>2</sub>RAQ, but undesirable when it causes saturation of the aromatic rings. The degree of ring saturation is very dependant on the reaction temperature, hydrogen pressure, and the degree of conversion (32,33). The hydroxyanthrone products (**XI**) and (**XII**) are tautomeric isomers of the anthrahydroquinone.

Anthrahydroquinone is structurally the aromatic analog of an enol whereas the hydroxyanthrone would be the ketone tautomer. The tautomerization process has been extensively reviewed (34). The rate of tautomerization is accelerated by acidic or basic surfaces, temperature, solvent polarity, and tautomer concentration (35). Each tautomer can be

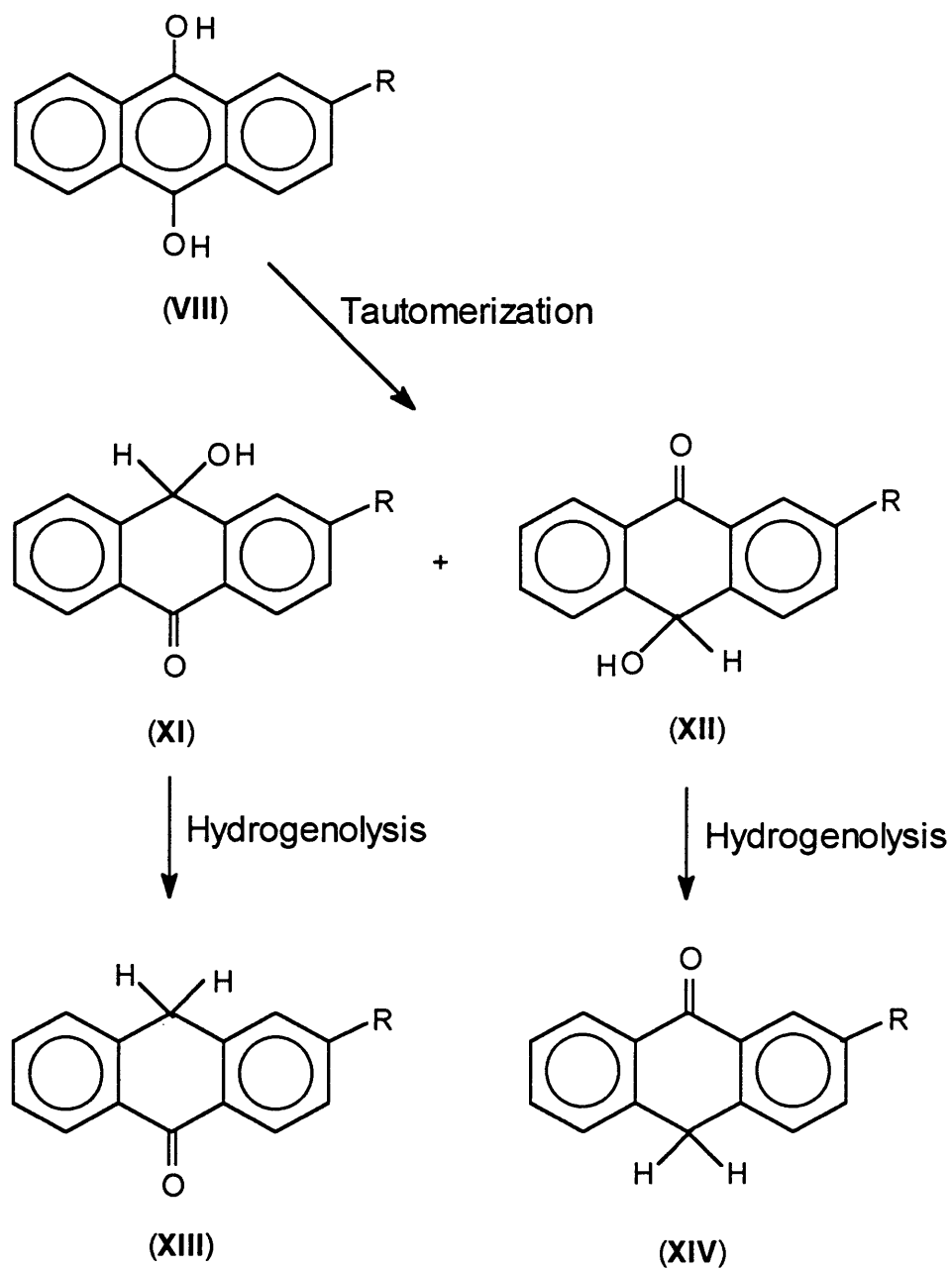


Figure 1b: Other possible side reactions occur in the autoxidation synthesis of  $\text{H}_2\text{O}_2$ .

isolated for extended periods of time if acid or base catalysts are rigorously excluded. While the equilibrium strongly favors the ketone over the enol form of non-aromatic tautomers, it does not with aromatic tautomers. In aromatic tautomers, the enol form will permit conservation of the aromaticity in the ring, and hence becomes more favored. For example, the equilibrium for the phenol-cyclohexadienone, (XV) and (XVI) respectively, tautomer system strongly favors the phenol tautomer (Figure 2).

Although supported Ni metal catalysts were used in the original anthraquinone autoxidation process, they exhibited excessive hydrogenation and hydrogenolysis. Therefore, prepoisoning of the nickel metal was often practiced to improve its selectivity (36). The fact that nickel was too sensitive to poisoning by oxygen and hydrogen peroxide led to the use of supported palladium, instead of nickel, in the process. The use of palladium improved the catalyst selectivity and durability (37,38).

## **2.6 Catalytic Hydrogenation of Aldehydes and Ketones**

The alkylanthrahydroquinone ( $H_2RAQ$ ) to be dehydrogenated in the HYSULF<sup>SM</sup> process contains aromatic hydroxyl groups, while the alkylanthraquinone product (RAQ)

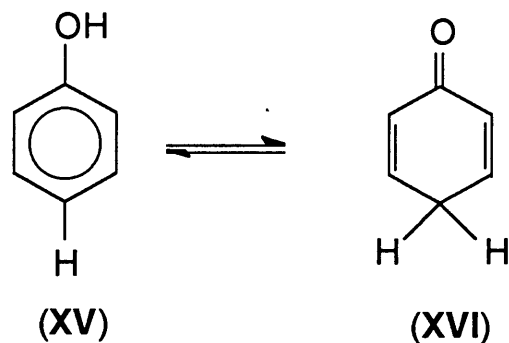


Figure 2: Phenol-cyclohexadienone tautomerization.

contains an aromatic carbonyl group. This chemical transformation is best described as a catalytic dehydrogenation of an alcohol. The catalytic dehydrogenation of alcohols to aldehydes and ketones by supported metals and metal oxides has been studied for decades (39,40,41,42,43). Typically, catalysts used for the hydrogenation of aldehydes and ketones are also considered to be good candidates for the dehydrogenation process (44,45). Presumably the dehydrogenation mechanism is the reverse of that for hydrogenation, though very little about the reverse process is known.

The catalytic hydrogenation of aldehydes and ketones into alcohols has been extensively reviewed (46). The use of supported platinum, palladium, Raney-nickel, cobalt, ruthenium, osmium, and copper chromite catalysts has been reported. Unfortunately, the hydrogenation of aromatic carbonyl groups is accompanied by ring saturation, C-O bond hydrogenolysis, and dehydration. Palladium metal is considered the best candidate for the hydrogenation of aromatic ketones to the corresponding alcohol with a minimum C-O bond hydrogenolysis (47,48). Copper chromite is the catalyst of choice when ring saturation is a problem. However, metal oxide catalysts usually require significantly higher temperatures and pressures for the hydrogenation reaction to occur. Supported rhodium catalysts give good results at mild reaction conditions (49,50,51). Hydrogenation over osmium is relatively slow, but it has higher product selectivity (52). The rate and selectivity of carbonyl hydrogenation are strongly affected by acidic or basic solvents and catalysts (53).

## **2.7 Hydrogenolysis of Aromatic Carbonyls**

As mentioned before, the most common byproducts of anthraquinone (**VII**) hydrogenation are the tetrahydroanthraquinone (**IX**), octahydroanthraquinone (**X**), hydroxyanthrones

(**XI**) and (**XII**), and anthrones (**XIII**) and (**XIV**) (see Figure 1). Hydrogenolysis of aromatic carbonyls is known to be easy, and is thought to occur via a benzylic alcohol intermediate (46). Since the hydroxyanthrones (**XI**) and (**XII**) are benzylic type alcohols, the C-O bonds are susceptible to hydrogenolysis. Therefore, anthrone formation is probably due to the hydrogenolysis of the C-O bond in hydroxyanthrones.

On the other hand, hydrogenolysis of C-C bonds is strongly affected by the type of metal, composition and crystallite size (54,55,56). A similar correlation between metal and C-O bond hydrogenolysis is also expected. For example, nickel and platinum usually show stronger C-C bond hydrogenolysis activity than does palladium. A similar relationship is observed in the hydrogenolysis of aliphatic C-O bonds. However, in the case of aromatic carbonyls, supported palladium catalysts also demonstrate high hydrogenolysis activity (57). Supported platinum or ruthenium catalysts are desired for unsaturated carbonyl compounds, where hydrogenation of the carbonyl is preferred.

Finally, there are important factors other than the catalyst that control the hydrogenolysis behavior. The

hydrogenolysis activity of the C-O bond is known to increase with an increase in solvent polarity, solvent acidity, reaction temperature, and hydrogen pressure (58).

## **2.8 Requirements of a Catalyst for HYSULF<sup>SM</sup> Process.**

A catalyst to be suitable for the HYSULF<sup>SM</sup> process has to be active and selective for the dehydrogenation of alkylanthrahydroquinone into alkylanthraquinone and hydrogen. Since the alkylanthraquinone is recycled in this process, selectivity is the more important factor in selecting or designing a catalyst. A small loss of the alkylanthraquinone reactant, through side reactions, during each cycle can severely limit the reaction efficiency. Selectivity is largely a function of the catalyst properties and can be managed to some extent by controlling the reaction temperature, space velocity, reaction pressure, and poisoning.

Metal and metal oxide catalysts have been widely applied for the dehydrogenation of alcohols and hydroquinones. Generally, in catalysis and especially in commercial processes, supported metal catalysts are preferred over the pure metal ones. This is due to the high cost and low surface area of the metals compared to the

cheap but high surface area of support materials. Actually, by supporting a metal, in a catalyst, a huge increase in the surface area is achieved at a relatively very low cost.

The lack of research in the area of anthrahydroquinone dehydrogenation means that substantial catalyst screening and catalyst design must be done. There is a significant volume of literature on the hydrogenation of anthraquinones and the dehydrogenation of alcohols. This information will be used along with some trial-and-error experiments to select catalyst candidates that are commercially available or to design new ones. Based on the available literature, supported metal, supported metal oxides, and pure metal oxide catalysts are the primary candidates.

A good catalyst for the HYSULF<sup>SM</sup> process should exhibit the following properties.

- It should have a good hydrogenation/dehydrogenation function. Metals such as platinum, palladium, and nickel are the best candidates for this function, but metal oxides, such as CuO and CeO<sub>3</sub>, have a relatively poor dehydrogenation ability and require higher temperatures for operation.
- The catalyst should not have any ring saturation activity.
- It should have little, or preferably no hydrogenolysis

activity. If possible, cleavage of the C-O bond must be eliminated. While metals have the most hydrogenolysis activity, metal oxides have the least.

- The catalyst support or the metal oxide should have a minimum Brønsted or Lewis acidity. Acidic or basic surfaces have the ability to convert the alkylanthrahydroquinone (an enol) into the keto tautomer. The keto tautomer is more easily converted into side products. This requires the use of neutral supports and avoidance of metal oxides that have multiple oxidation states.

- The catalyst should have good tolerance to sulfur poisoning due to the possibility that traces of sulfur may be present in the feedstock. Platinum metal has better tolerance than palladium or nickel metals, and chromia ( $\text{Cr}_2\text{O}_3$ )-based catalysts have better tolerance than copper oxide.

- The catalyst has to be of high activity. This requires high dispersion of the active metal sites on the surface. Unfortunately, the best catalyst supports are also highly acidic. At the same time, pore and film diffusion should be minimized if possible.

Finding a catalyst that meets all of the above criteria is very difficult. The purpose of this study is to

identify, or design, the best catalyst candidate and to determine the optimum operating conditions for that catalyst. In addition, the details of the catalyst surface mechanism will be investigated.

## CHAPTER 3

### STATEMENT OF THE PROBLEM

In a refinery, petroleum distillates contain sulfur-containing compounds which are converted to hydrogen sulfide during the reforming process. Hydrogen is a valuable product in the refining industry and is often in short supply. Hydrogen sulfide, if it can be utilized, is a potential source of hydrogen. Nowadays all industrial refining processes convert hydrogen sulfide into elemental sulfur and water, thus eliminating a potential source of hydrogen.

The only catalytic process to convert hydrogen sulfide into hydrogen and elemental sulfur at moderate temperatures is the HYSULF<sup>SM</sup> process (13). The fundamental chemistry of this process is not totally understood. A better understanding of the reaction chemistry is required for the process to be successfully commercialized.

The objectives of this study are:

1. To test commercially available catalyst candidates for the dehydrogenation of 2-t-butyl-9,10-dihydroxyanthracene ( $H_2TBAQ$ ) to 2-t-butyl-9,10-anthraquinone (TBAQ) and hydrogen.
2. To design and test new candidate catalysts. In either case, the catalysts should have good selectivity and activity for the conversion of 2-t-butyl-9,10-dihydroxyanthracene ( $H_2TBAQ$ ) to 2-t-butyl-9,10-anthraquinone (TBAQ) and hydrogen.
3. To optimize the catalyst selectivity and activity by varying the reaction conditions. This requires the design of a testing sequence which observes the effects of temperature, pressure, flow rate, catalyst particle size, and catalyst formulation on its activity and selectivity for the dehydrogenation reaction. At the same time, the effect of catalyst poisoning, catalyst pretreatment and feed additives on catalyst activity and selectivity will be studied.
4. To understand the fundamental chemistry of the surface reactions. This objective will be fulfilled by studying the

results obtained from product analysis and catalyst characterization. Nuclear magnetic resonance spectroscopy will be used to determine the product distribution in the liquid phase. Gas chromatography will be applied to the analyses of the gaseous products. Catalyst characterization techniques such as X-ray diffraction, BET surface area determination, and carbon monoxide chemisorption will also be used to study the bulk and surface properties of selected catalysts before and after a testing sequence.

## CHAPTER 4

### EQUIPMENT AND EXPERIMENTAL PROCEDURES

#### 4.1 Chemicals Used

All materials were used as received unless otherwise stated.

##### 4.1.1 Feedstock and Treatment Chemicals

N-Methyl-2-pyrrolidinone (NMP) practical grade was obtained from J. T. Baker. 2-t-Butyl-9,10-anthraquinone (TBAQ; 98%), cyclopentene (97%), and methylsulfide were purchased from Aldrich. Hydrogen sulfide CP grade (99.3%) was supplied by Air Products Company. Industrial- (99.98%) and zero-grade (99.995%) nitrogen and technical-grade helium (99.95%) were purchased from General Air Service and Supplies.

##### 4.1.2 Chemicals Used in Catalysts Preparation

Platinum(IV) chloride ( $\text{PtCl}_4$ ; 98%) and tetraammine-palladium(II) nitrate ( $\text{Pd}(\text{NH}_3)_4\text{NO}_3$ ) was supplied by Aldrich. Tetraamminepalladium(II) nitrate ( $\text{Pd}(\text{NH}_3)_4(\text{NO}_3)_2$ , containing 35.61% Pd) was purchased from Strem Chemicals. Palladium

(II) chloride ( $\text{PdCl}_2$ ) was obtained from Engelhard Company. Rhodium(III) chloride trihydrate ( $\text{RhCl}_3 \cdot 3\text{H}_2\text{O}$ ) was obtained from Fisher Scientific, while palladium/gold alloy disk (30 wt% Pd, 70 wt% Au) came from Denton Vacuum. Lanthanum (III) nitrate hexahydrate ( $\text{La}(\text{NO}_3)_3 \cdot 6\text{H}_2\text{O}$ ) was purchased from Alfa Products and Fisher Scientific companies. The catalyst supports used were silica ( $\text{SiO}_2$ , grades 57 and 3) which were provided by Davison, and magnesium oxide ( $\text{MgO}$ ) was provided by Harshaw. The quartz support was prepared by crushing amorphous quartz glass obtained from Allen Scientific (Boulder, Colorado) to the desired particle size.

#### **4.1.3 Commercial Catalysts**

Two commercial catalysts were tested. These were Cyanamid Aeroform<sup>R</sup> PHF-4 platinum reforming catalyst 0.8% Pt on alumina (American Cyanamid Company), and chromium oxide on alumina, 12% Cr as  $\text{Cr}_2\text{O}_3$ , (Strem Chemicals). These catalysts were crushed and sieved to the desired mesh sizes, followed by pretreatment using the same methods as will be discussed for the catalysts synthesized in this study.

#### **4.1.4 Catalysts Prepared by Previous Graduate Students**

These catalysts were 2.75%Pt/2.50% $\text{La}_2\text{O}_3$ /SiO<sub>2</sub> grade 57 with a mesh size of 14-30 (1.40-0.60 mm), and the

2.75%Pt/5.00%La<sub>2</sub>O<sub>3</sub>/Al<sub>2</sub>O<sub>3</sub> with a mesh size of 14-30 (1.40-0.60 mm) (59).

#### **4.2 Feedstock Preparation and the Glass Reactor Setup**

Feedstock solutions were prepared using a mini-glass reactor. Figure 3 illustrates a schematic picture of this reactor. The glass reactor consists of a 500 ml glass bottle, capable of holding pressures of 50-60 psig, which can be sealed to a stainless steel manifold using a silicone or rubber O-ring. The bottle was immersed in a hot water bath heated by a hot plate. The water bath and the feedstock temperatures were maintained at 50°C using a temperature controller. The temperatures of the water bath and the reaction mixture were measured using K-type thermocouples and displayed on an Omega temperature indicator.

A 1/16" K-type thermocouple and two 1/16" stainless steel tubes were passed through a 1/4" stainless steel tube to the lower third of the glass reaction vessel. One of these two 1/16" stainless steel tubes served as the gas inlet and has a sparger at its end. The purpose of the sparger was to introduce the inlet gases into the reaction mixture as small bubbles. This process increased the

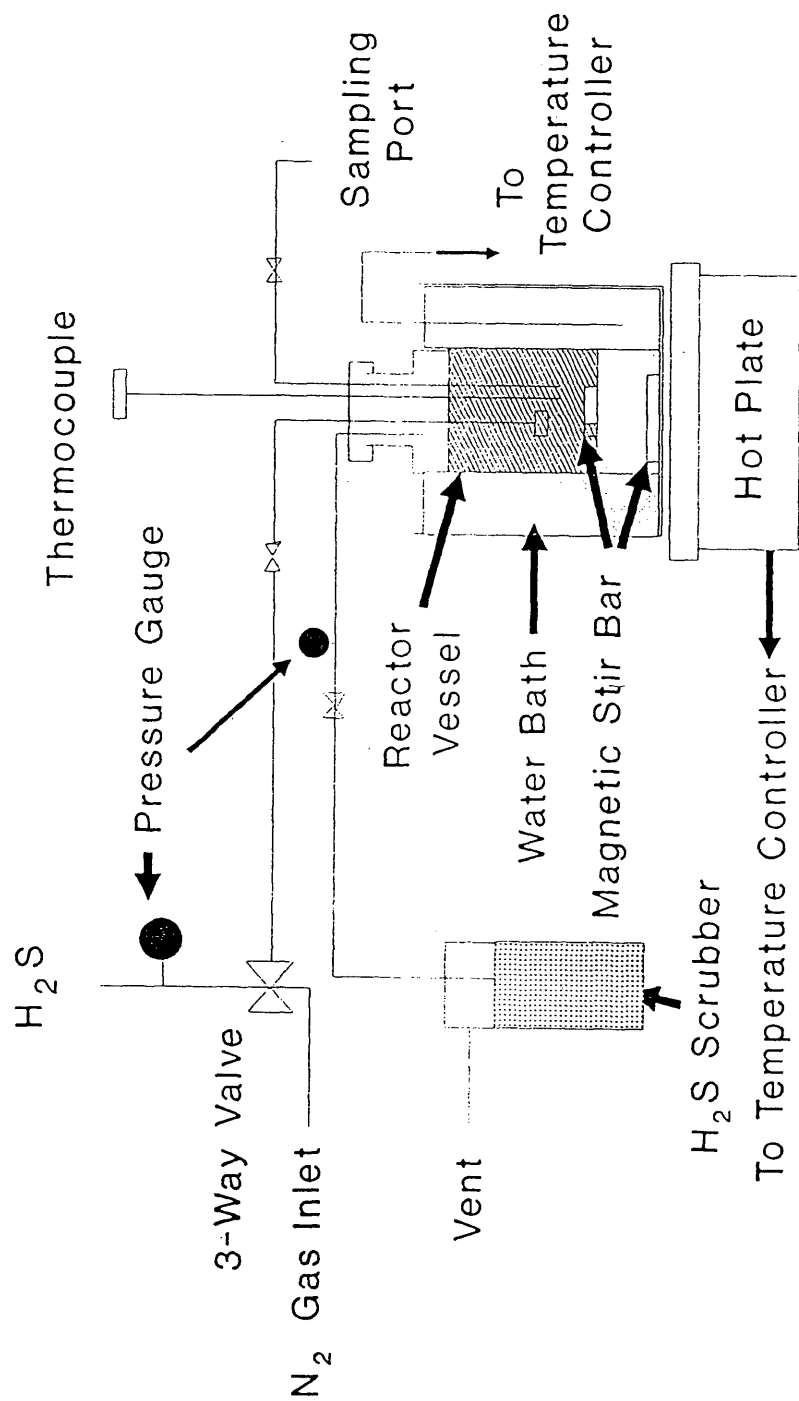


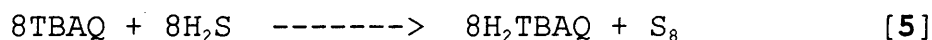
Figure 3: The glass reactor used in the preparation of the catalyst feed.

contact between the gas and the reaction mixture by increasing the surface area of the inlet gas bubbles. The second 1/16" tube was connected to a two-way valve and served as a sampling outlet to collect liquid samples of the reaction mixture to be analyzed during the reaction.

The outlet of the reaction vessel was a 1/4" stainless steel tube attached to a Swaglock tee connector. One arm of this tee was connected to a pressure gauge to monitor the pressure inside the reaction vessel while the other arm served as the gas outlet. The gas outlet tube was connected to a series of gas scrubbers containing 3 M solutions of sodium hydroxide (NaOH) to remove the unreacted H<sub>2</sub>S gas exiting the reactor. In these NaOH solutions, H<sub>2</sub>S gas was converted into a non-volatile NaHS salt soluble in the aqueous medium. The water bath and the reaction mixture were stirred using Teflon-coated magnetic bars.

A solution of TBAQ in NMP (25% wt TBAQ) was placed in the reaction vessel. The glass vessel was then connected to the steel reactor manifold, placed in the hot water bath and stirred. The solution mixture was purged with nitrogen gas (99.98%; at 15-25 psig pressure) for 10 minutes to drive off dissolved air. The temperature of the water bath and the

reaction mixture were kept constant at 50°C. H<sub>2</sub>S gas was introduced into the reactor and the solution was purged for 10 to 15 minutes to drive off any trapped nitrogen gas. The outlet valve was then shut off and the H<sub>2</sub>S inlet valve was kept open. The H<sub>2</sub>S pressure in the reaction vessel was maintained at 40 psig. Within 30 minutes of reaction, solid sulfur particles could be seen in the reaction solution according to the following reaction (see Equation [5] in Chapter 2).



After 6 hours the reaction was stopped, the hot water bath was replaced by an ice bath, and the reaction mixture was cooled to 0°C. Unreacted H<sub>2</sub>S was released slowly to the gas scrubbers and the mixture was purged again with nitrogen to drive off residual H<sub>2</sub>S. The precipitated sulfur was vacuum filtered using a 10-15 μm porosity centered-glass funnel. The product mixture containing H<sub>2</sub>TBAQ, unreacted TBAQ, and residual dissolved sulfur in NMP was placed overnight in a freezer to allow residual sulfur, in the solution, to precipitate.

The next day, the frozen solution was allowed to melt and the sulfur precipitate was vacuum filtered using a Millipore 10  $\mu\text{m}$  membrane filter. The filtrate was poured into the 500 mL reactor vessel. The vessel was connected to the set-up described and placed in a mineral oil bath. The solution was kept at 135°C, continuously purged with nitrogen, and stirred for 3 hours in order to strip off residual  $\text{H}_2\text{S}$ . Finally, the solution was cooled to room temperature and used as a feedstock for the catalytic dehydrogenation step.

### **4.3 Catalyst Preparation**

#### **4.3.1 Catalyst Supports**

Catalyst supports used were either as received or after surface treatment and preparation.

##### **A. Untreated Supports**

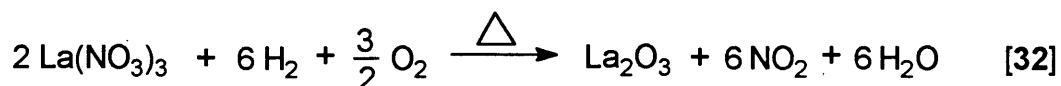
The untreated support materials were silica ( $\text{SiO}_2$ ) grade 57 (99.5% wt.  $\text{SiO}_2$ ; 300  $\text{m}^2/\text{gm}$  surface area; 1.0 cc/gm pore volume; and 0.40 gm/cc packed density) of 8 mesh size (Davison), and magnesia ( $\text{MgO}$ ) (99.8% wt.  $\text{MgO}$ ; 21  $\text{m}^2/\text{gm}$  surface area; 0.20 cc/gm pore volume) tablets of 1/8" diameter (Harshaw). All support materials were crushed, sieved to the desired mesh sizes, and calcined overnight at

500°C under vacuum to remove adsorbed water.

### **B. Treated Supports**

The surface chemical properties of the support materials were modified by doping them with  $\text{La}_2\text{O}_3$ . This treatment enhances the dispersion of the metal crystallites on the support surface and reduces the support acidity. Support materials were crushed, sieved to the desired mesh sizes, and calcined overnight at 500°C under vacuum. While still under vacuum, the support material was then cooled to room temperature. Using the incipient wetness technique, the support material was impregnated with an aqueous solution of  $\text{La}(\text{NO}_3)_3$  (59,60,61).

This technique involves the addition of an aqueous solution of  $\text{La}(\text{NO}_3)_3 \cdot 6\text{H}_2\text{O}$  that is sufficient to fill the pores and wet the surface of the calcined support. The desired weight percent of  $\text{La}_2\text{O}_3$  was obtained using a stoichiometric amount of lanthanum nitrate. Note that for each mole of the oxide, 2 moles of the nitrate are needed (see Equation [32]). The solution was then prepared by dissolving this stoichiometric amount of the nitrate salt in an amount of water sufficient to fill the pores and wet the support surface.



This amount of water was determined by the wettability of the support material and the support weight. The support wettability was determined as follows:

1. A certain amount of the cold calcined support was weighed exactly on an analytical balance.
2. Deionized water was added dropwise with continuous shaking and mixing to the support until the particles became wet and started to coagulated (or cling together) and became like a moistened amount of sugar or salt.
3. The wet mixture was reweighed, and the weight of water was then determined by difference.

The wettability of the support was then determined by dividing the weight of water by the weight of the dried calcined support used, i.e. gm H<sub>2</sub>O/gm of support. After impregnating the support with the aqueous lanthanum nitrate solution, the wet mixture was dried with air flow for 2-3 hours at temperatures > 100°C and then calcined overnight in vacuum at 500°C.

### 4.3.2 Supported Metal Catalysts

#### A. Lanthana-Doped Catalysts on Silica Grade 3

Catalysts of palladium (Pd), platinum (Pt), and rhodium (Rh) on lanthanum oxide (lanthana,  $\text{La}_2\text{O}_3$ )-doped silica ( $\text{SiO}_2$ ) grade 3 were prepared and tested. The general procedure used to prepare these catalysts was as follows: the support materials were crushed to the desired mesh sizes, sieved, placed in an evaporating dish and calcined overnight at  $500^\circ\text{C}$  under vacuum. On the next day, the support was cooled, under vacuum, to room temperature and weighed.

To the preweighed support material in the evaporating dish, the corresponding amount of a solution of lanthanum(III) nitrate hexahydrate ( $\text{La}(\text{NO}_3)_3 \cdot 6\text{H}_2\text{O}$ ) was added dropwise. During the addition of the solution to the support, continuous mixing and shaking of the combined mixture was performed. The amount of water used in the preparation of the solution was determined by multiplying the wettability of the support ( $\text{gm H}_2\text{O}/\text{gm support}$ ) by the support weight. The wet mixture was then dried at  $110\text{-}120^\circ\text{C}$  with a flow of air for 2-3 hrs and then calcined again at  $500^\circ\text{C}$  overnight under vacuum. The following day, the mixture was cooled under vacuum to room temperature.

An aqueous solution of the desired metal salt was then added dropwise to the calcined-doped support with continuous shaking and mixing. The continuous stirring was necessary to obtain homogeneity and maximum dispersion of the metal salt on the treated support. The metal salt solution was prepared using a calculated weight of the salt required to yield the desired weight percent of the pure metal per gram of doped support. Here again, the amount of water used in preparing the metal solution was the same as that required, before, to wet and fill the support surface and pores.

The metal-impregnated wet mixture was then dried, as above, at 110-120°C with a flow of air for 2-3 hrs. The mixture was again calcined overnight under vacuum at 500°C. On the next day, the calcined catalyst was cooled to room temperature in a desiccator and stored in an air-tight vial which was placed in a desiccator for future use.

The use of lanthanum and metal nitrate salts, if possible, is favored over chloride or other halogen salts. This is due to the fact that, when calcined, the nitrate group produces  $\text{NO}_2$  gas which will leave the catalyst structure. This results in obtaining a catalyst almost free from any acidic properties. On the contrary, when halide

metal salts are used residual anions ( $\text{Cl}^-$ , etc.) remain within the catalyst structure giving the catalyst some acidic properties.

Unfortunately, the use of non-halogen salts was not always possible due to availability or solubility reasons. In these cases, the use of halo metal salts becomes the only choice. Catalysts of this type were of 2.50-2.75% metal/5.00%  $\text{La}_2\text{O}_3/\text{SiO}_2$  Grade 3, namely, 2.50% Pd/5.00%  $\text{La}_2\text{O}_3/\text{SiO}_2$  Grade 3; 2.50% Rh/5.00%  $\text{La}_2\text{O}_3/\text{SiO}_2$  Grade 3; and 2.75% Pt/5.00%  $\text{La}_2\text{O}_3/\text{SiO}_2$  Grade 3. The salts of the metals used were  $\text{Pd}(\text{NH}_3)_4\text{NO}_3$ ,  $\text{RhCl}_3 \cdot 6\text{H}_2\text{O}$ , and  $\text{PtCl}_4$ .

#### **B. Lanthana-Doped Catalysts on Silica Grade 57**

These catalysts were prepared in the same way used in Section **A** with one exception where the support was the less acidic silica grade 57. Several catalysts of 2.75% Pt/2.50%  $\text{La}_2\text{O}_3/\text{SiO}_2$  Grade 57 with three different particle sizes where the particle size was reduced approximately by 50% every time they were prepared. These sizes were 1.40-0.84 mm and approximately 0.70-0.42 mm and 0.42-0.21 mm. These catalysts were tested at different dehydrogenation conditions such as temperature, pressure, and flow rates of the hydroquinone feed solution with and without additives.

A palladium catalyst on the same doped support, namely 2.75% Pd/2.50% La<sub>2</sub>O<sub>3</sub>/SiO<sub>2</sub> Grade 57, was also prepared and tested at different reaction conditions.

### **C. Lanthana-Doped Catalysts on Quartz**

Platinum on lanthana-doped quartz catalysts were prepared and tested. The methods of preparation for these systems were slightly different. The first catalyst 2.75% Pt/2.50% La<sub>2</sub>O<sub>3</sub>/quartz, was prepared using a slightly different approach. Due to the fact that quartz is almost a non-porous material, its surface area is very small, hence, its wettability is very low. Since the amount of water required to wet the quartz surface was not enough to dissolve the required weight of PtCl<sub>4</sub>, a solution of the metal salt was prepared using an amount of water that just dissolved the salt. A portion of the solution was added dropwise to the calcined quartz which was then dried and calcined in the same way as the other catalysts. After cooling this partially impregnated catalyst, the second portion of the platinum chloride solution was added dropwise to the quartz and then treated in the same way as before. The ready double impregnated catalyst was finally put in a vial and stored in a desiccator for further use.

For the second catalyst of this type, in order to use a small amount of water to prepare the metal solution, the amount of  $\text{PtCl}_4$  was reduced. Hence, the support was impregnated only once with the metal salt solution. The catalyst prepared using this approach was 0.50% Pt/2.50%  $\text{La}_2\text{O}_3$ /quartz. Since large surface areas of the catalysts are desired, the small surface area of quartz can be considered as a disadvantage. However, this disadvantage in surface area can be minimal when the low surface acidity of quartz is considered. The low acidity was the reason behind the preparation of this type of catalyst. The doping with lanthana was supposed to enhance the metal dispersion on the low surface area quartz.

#### **D. Undoped Catalysts**

These catalysts were prepared using the same impregnation technique mentioned in Sections **A** and **B**. The only difference in preparation between these catalysts and the ones mentioned in Sections **A** and **B** was that no dopant was used, hence, the metal was directly impregnated to the support. Two platinum-based catalysts of this type were prepared and tested. The first was 2.75%Pt/ $\text{SiO}_2$  grade 57 with a particle size of 0.70-0.42 mm. The second was 2.75%Pt/MgO and of the same particle size.

### **E. Electrospattered Catalyst**

The treated support of this catalyst was some of the 2.50% La<sub>2</sub>O<sub>3</sub>/quartz which was prepared in Section C. The metals were loaded on the treated support using a vacuum sputtering technique. A disk of Pd/Au alloy was placed in an electrospattering instrument. The support material was placed in a small dish inside the instrument. The instrument vessel, containing the disk and the support, was then evacuated. The support was then sputtered several times with the alloy material. Very short periods (msec periods) of discharge were applied. The catalyst was then used in the same manner as the rest of the catalysts tested in this research.

### **4.4 Catalytic Reactor**

An up-flow 316 stainless steel catalytic reactor was used in this investigation. The schematic drawing of the catalytic reactor is shown in Figure 4. The reactor consisted of a 1/2" stainless steel tube. At the bottom, this 1/2" tube was connected to a coiled 1/16" stainless steel tube which served as the reactor inlet and a preheater for the catalyst feed. At the top, the reactor was connected to a 1/4" stainless steel tube which acted as the reactor outlet. A J-type thermocouple was located at the

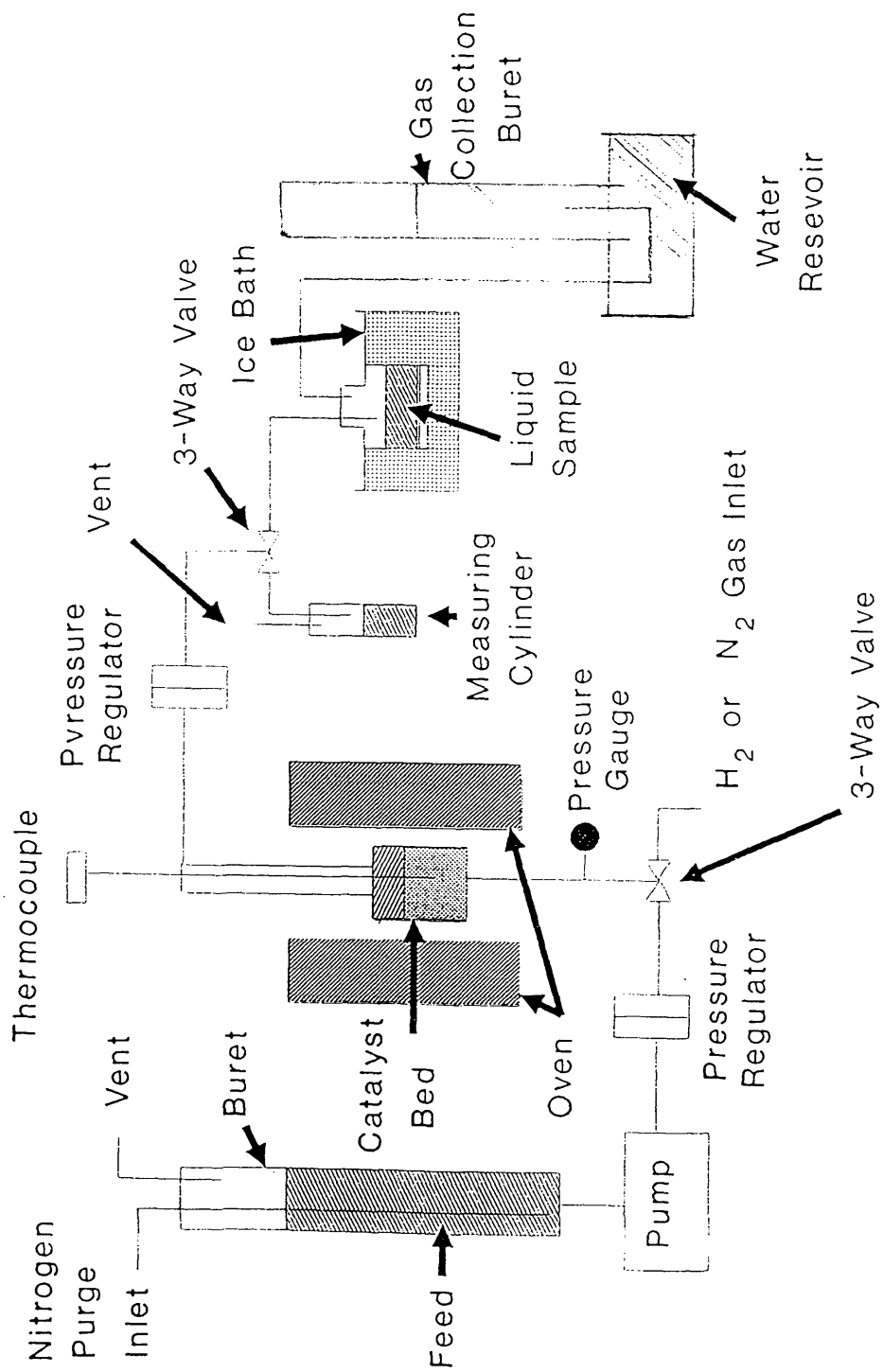


Figure 4: The stainless steel catalytic reactor.

center of the catalyst bed and connected to an Omega digital temperature indicator to monitor the catalytic reaction and the catalyst bed temperature. The temperature of the catalyst bed was regulated by a Lindberg electric furnace with a J-type thermocouple inside its walls touching the reactor walls. The thermocouple was connected to an Omega temperature controller. The pressure inside the reactor was controlled by a Mity-Mite back pressure regulator. The outlet of the Mity-Mite regulator was connected to a three-way valve which diverted the product mixture to either a calibrated cylinder or an ice-cooled sample collection bottle. The calibrated cylinder was used to monitor and measure the liquid flow rate.

The pre-weighed catalyst, about 0.500 gm, was packed into the 1/2" reactor tube with a layer of glass wool at the bottom and another at the top of the catalyst bed. The reactor was then sealed, placed in the furnace, purged with nitrogen gas followed by hydrogen, and then pressurized with hydrogen at room temperature. The purpose of pressurizing the reactor with hydrogen was to check for leaks which was achieved using a commercially available combustible gas detector. The pressure was then released and a continuous hydrogen flow of 40 mL/min was maintained.

Within one hour, the temperature of the furnace was gradually increased from room temperature to 450°C which was maintained for two more hours to reduce the catalyst. The catalyst was then cooled to room temperature and kept under a slight hydrogen pressure until the dehydrogenation test.

Before introducing the reaction feed to the catalyst, the catalyst was heated to about 180°C and purged continuously with zero-grade nitrogen gas for 20-30 min. The nitrogen flow was then stopped, and the feedstock containing 25 wt% of H<sub>2</sub>TBAQ and TBAQ in NMP solvent was introduced to the catalyst by means of a dual double-cylinder Milton Roy mini pump. The flow rate capacity of the pump was 29-290 mL/hr, with a maximum pumping pressure of 5000 psig. A Mity-Mite pressure regulator was attached to the pump outlet line. A constant back pressure of nitrogen, working against the pump produced a constant liquid flow rate.

By selecting the appropriate liquid flow rate and the catalyst bed volume, the desired residence time of the reaction mixture in the catalyst bed was controlled. The pressure inside the reactor was maintained by a pressure regulator and monitored by means of a pressure gauge

connected to the inlet tube of the reactor. Depending on the purpose of the test, the pressure inside the reactor was kept in the range of 10-107 psig and was always kept above the vapor pressure of the NMP solution at the reaction temperature which avoided any loss of the solvent due to evaporation.

Both liquid and gaseous reaction products were passed through a 1/8" stainless steel tube attached to a stainless steel needle penetrating through a rubber septum of a serum bottle kept at 0°C in an ice bath. The liquid product was collected in the serum bottle while the hydrogen gas was allowed to escape from the serum bottle by means of a second needle connected to a collection buret in which the volume of the hydrogen produced was measured.

The void-volume in the reactor tube above the packed catalyst bed was minimized by adding small-size glass beads. This reduction in the void-volume reduced the residence time of the reactants and products in the hot zone of the reactor after leaving the catalyst bed, thus, minimizing undesirable thermal reactions.

#### **4.5 Analytical Equipment**

The following analytical techniques and equipment were used to analyze the reaction products and to characterize the catalysts before and after each test to get an idea about the feasibility of the catalytic test performed.

##### **4.5.1 Nuclear Magnetic Resonance (NMR)**

Two NMR instruments were used to analyze the composition of the feedstock and reaction products. By knowing the mole percents of H<sub>2</sub>TBAQ, TBAQ, and any other possible quinone species before and after each reaction run, one can calculate the efficiency for that particular test. This information will lead to various modifications of the dehydrogenation tests in order to increase the efficiency, selectivity and activity of the catalyst, and minimize the production of undesired products.

During the first stages of this project, a Varian EM 390, 90 MHz NMR instrument was used to analyze the composition of the feedstock and reaction products. The intensity of the proton peaks in the aromatic region were initially used to calculate the relative percentages of the H<sub>2</sub>TBAQ and TBAQ present. Multiple peaks in the t-butyl group region for TBAQ suggested the presence of side

products which was impossible to be identified in the aromatic region due to mixing with other relatively similar aromatic compounds present like the TBAQ and H<sub>2</sub>TBAQ. It was then became obvious that the 90 MHz instrument had insufficient resolution to provide good enough quantitative data from its spectrum.

Therefore, most of the quantitative analyses were performed on a 300 MHz Fourier transform General Electric NMR instrument. The new instrument gave very good quantitative analysis in the t-butyl region of the spectra which was used exclusively in the determination of each quinone species present.

#### **4.5.2 X-Ray Diffraction (XRD)**

Two x-ray diffraction instruments were used to get XRD diffraction measurements of the catalysts used before and after testing. The first was a Rigako Vertical Rotaflex RU 200 with a Cu K $\alpha$  (1.54098 Å) radiation source at 40 kV power and 40-70 mA current. Catalyst samples were ground to a very fine powder using a marble agate mortar and pestle. Disks of powdered samples were prepared and the spectra were recorded for 2 $\theta$  values from 10° to 90°. The second instrument was a powder diffraction unit.

The x-ray reflection data were collected as ASCII files which were manipulated and graphed using Sigma Plot software. From the plotted data, peak widths were calculated for each spectrum. The peak widths of the tested catalysts were compared with those of the untested fresh catalysts. These data gave information about the metal dispersion and if the metal crystallites underwent any changes such as centering, migration, or poisoning during the dehydrogenation reaction.

Using well known mathematical correlations (see Equation [38]), the crystallite size of the metal on the support surface could be calculated. These data, along with other information obtained from testing, can lead to the possible causes of catalyst deactivation and assisted in the prediction of catalyst durability and lifetime under the reaction conditions.

#### **4.5.3 Gas Chromatography (GC)**

Two gas chromatography instruments were used. The first one was a Varian Aerograph series 2800 with a stainless steel column packed with Porepack Q. Zero grade nitrogen gas (99.995%) was used as the carrier at a flow rate of 40 mL/min. Two milliliter samples of the collected

gas were injected to the instrument using a gas tight syringe. All samples analyzed showed that hydrogen gas was the major product. Detailed analyses were done on another instrument and gave hydrogen gas as the main product. Trace amounts of hydrocarbon species were also detected in the products of some of the catalyst tests.

#### **4.5.4 Gas Chromatography/Mass Spectrometry (GC-MS)**

An Extrel ELQ 400 triple quadrupole mass spectrometer interfaced to a Varian 3400 gas chromatograph with a (J & W DB-5) column 30 m in length, 0.32 mm ID and a film thickness of 0.25  $\mu\text{m}$  was used for analysis of the less volatile compounds. A 0.5  $\mu\text{l}$  volume of the reaction products was introduced to the injection port; the column was heated from 50°C, with a 2 minute initial hold, to 250°C, with a final 5 minutes hold, at a heating rate of 6°C/min. The mass spectrum was scanned from 35 to 350 amu at a rate of 475 amu/sec. The source temperature was 220°C and the interface was 280°C. Unfortunately, the high temperature conditions used in the injection port resulted in some thermal decomposition products in addition to the original reaction products.

#### **4.5.5 Thermal Gravimetric Analysis (TG/DTA)**

A TG/DTA 320 Seiko thermal analysis system was used to determine the amount of carbon deposit, if any, on the tested catalysts. Nitrogen gas or air were used at a flow rate of 300 ml/min. Samples were heated to 230°C and held for 10 minutes with nitrogen flow to remove residual solvent present (boiling point of NMP is 206°C). An air flow was then started and the temperature was raised from room temperature to 230°C at a rate of 20°C/min with a hold of 10 minutes at 230°C, and then from 230°C to 500°C at a rate of 10°C/min with a final hold of 15 minutes at 500°C to insure that all the carbon deposit was burned off. A thermogram and the sample weight losses were recorded.

#### **4.5.6 Surface Area**

Using the multi-point B.E.T method, the total surface area, pore size, and pore volume of selected catalysts were determined before and after testing. This method is the most commonly used method for measuring the total surface area of catalysts (64).

A commercially available automated gas adsorption instrument was used. Nitrogen gas was used as an adsorbate in a method based on the ASTM method number D 1993-91 (65).

#### 4.5.7 Specific Metal Surface Area (Chemisorption)

The determination of the specific metal surface area provides information about exposed metal surface area and/or concentration of the active metal sites per gram of catalyst. Information regarding changes in the number of active metal sites can be obtained by comparing the chemisorption results of the fresh and tested catalysts.

Samples of the selected catalysts were placed in a clean, preweighed sample glass tube. The tube was attached to the instrument and purged with hydrogen gas at a preselected flow rate. Using a heating mantle, the temperature was increased from room temperature to 450°C. The catalyst was reduced with hydrogen at 450°C, then flushed with helium gas at the same temperature. Finally, the mantle was removed and the sample under helium gas was cooled to room temperature.

A known volume of CO was injected into the sample tube with the excess CO vented through an on-line gas chromatograph. A chromatogram was obtained and the amount of the nonsorbed CO was determined from it. In the second test, a sample of CO with the same volume as before was injected again onto the catalyst and a second peak in the

chromatogram was obtained. The tube was then removed and quickly weighed using an analytical balance. Assuming that a negligible weight of CO had been adsorbed, the weight of the catalyst was obtained from the difference in weight between the tube with the catalyst and that of the empty tube. The amount of CO ( $\mu$  moles) was then calculated using the difference between peak area of the second peak on the chromatogram (no chemisorption) and that of the first GC peak (CO adsorption). Theoretically, the chemisorption of CO on silica is negligible compared to that on the metal sites (3). Assuming that every CO molecule is adsorbed on a single metal site, the number of moles of the metal active sites was the same as the number of moles of CO adsorbed.

#### **4.5.8 Chloride Analysis**

Due to the fact that support acidity affects the catalyst selectivity in this process by increasing the chance for the undesired hydrogenolysis reaction of the C-O to take place, chloride analysis was done to know how much chloride ions were present per gram of catalyst. The presence of chloride ions increases the acidity of the catalyst through the formation of HCl. The hydrogen used in the formation of this HCl is easily that present on the SiO<sub>2</sub> surface. This acidity leads to the dehydration of the OH in

H<sub>2</sub>TBAQ. So, a few selected catalysts were analyzed to determine their chloride ion content in order to correlate it with the extent of the hydrogenolysis reaction.

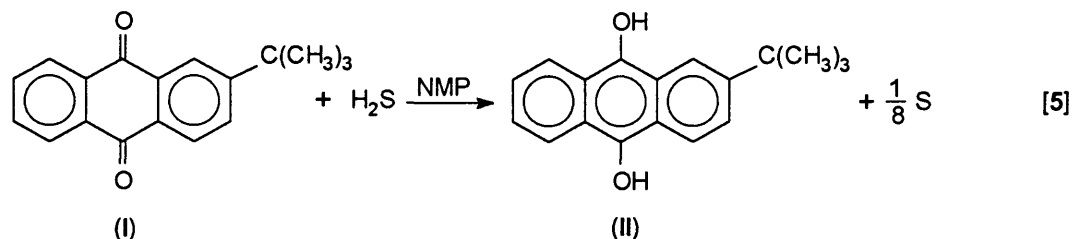
## CHAPTER 5

### RESULTS and DISCUSSION

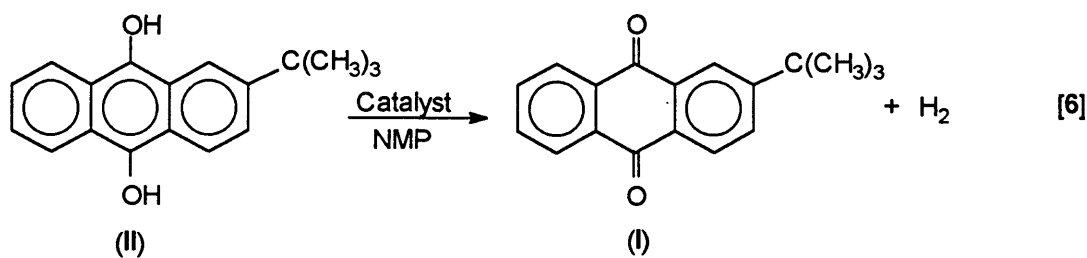
#### 5.1 General Overview

The subject of this document, the HYSULF<sup>SM</sup> desulfurization process, consists of two stages. In the first stage 2-t-butyl-9,10-anthraquinone, TBAQ (**I**), dissolved in N-methyl-2-pyrrolidinone (NMP) is reacted with H<sub>2</sub>S to produce 2-t-butyl-9,10-dihydroxyanthracene, H<sub>2</sub>TBAQ (**II**), and elemental sulfur (see Section 4.2, or 2.4 and Equation [5]). NMR spectroscopic analyses of the products of this reaction showed proton signals that correspond to TBAQ and H<sub>2</sub>TBAQ. No other quinone products were obtained from this hydrogenation reaction. The second stage (see Section 4.4 and Equation [6]) involves the catalytic dehydrogenation of H<sub>2</sub>TBAQ (**II**) to produce the original TBAQ (**I**) and molecular hydrogen.

In general, a heterogeneous catalyst consists of one or more of the following, a support material, a dopant, and a metal crystallite(s). In this study all the catalysts used were supported metal or metal oxides. Both doped and



NMP = N - Methyl - 2 - pyrrolidinone



undoped supports were used in catalyst preparation (see Chapter 4). A catalyst can increase the reaction rate of a certain chemical process without interfering with the process thermodynamics. The increase in reaction rate is obtained by providing alternative reaction pathways and kinetics.

In this study, the two catalytic reaction products were collected in two different physical phases and analyzed. TBAQ (**I**) was collected as a solution in NMP (the liquid portion of the products) and produced hydrogen was collected as gas in the gas collection vessel (see Section 4.4). Since the catalytic reaction was performed at a relatively elevated temperatures ( $> 200^{\circ}\text{C}$ ) in the presence of support materials which can be acidic or basic in behavior, products other than TBAQ (**I**) were expected to form. Analyses of the liquid portion of all catalyst screening tests showed the presence of TBAQ as the main reaction product. On the other hand, the analyses of some of these liquid portion products showed the presence of byproducts in addition to the major TBAQ product. Under the catalytic reaction conditions applied in this study and in comparison with the available literature, the most likely quinone byproducts to be present are: 2-t-butyl-9-hydroxyanthrone (**XVII**), (TBHOAN 1); 2-t-butyl-10-hydroxyanthrone (**XVIII**), (TBHOAN 2); 2-t-butyl-9-hydroxyanthracene (**XIX**), (TBANOL 1); 2-t-butyl-10-hydroxyanthracene (**XX**), (TBANOL 2); 2-t-butyl-9-anthrone (**XXI**), (TBAN 1); and 2-t-butyl-10-anthrone (**XXII**), (TBAN 2). Figure 5 shows the chemical structures of these compounds.

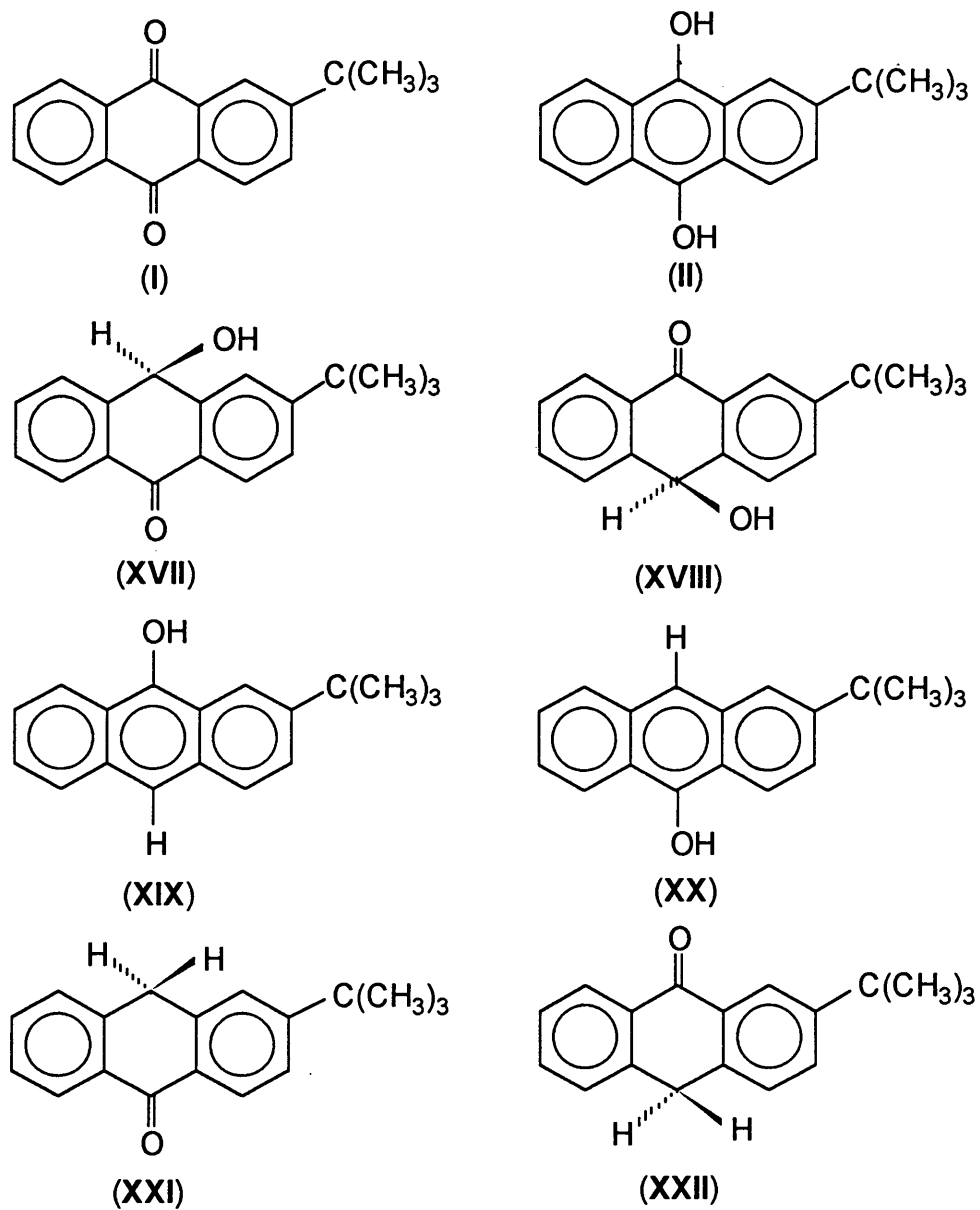


Figure 5: Possible quinone derivatives present in the catalytic reaction product mixtures.

One of the goals of this study was to identify and/or prepare and test a catalyst(s) that would be suitable for the dehydrogenation of  $H_2TBAQ$  (**II**). Several catalysts were tested under a variety of reaction conditions. In order to evaluate a tested catalyst, specific information about its performance, behavior, and durability during the intended reaction and operating conditions must be known. Therefore, as a minimum, a knowledge of the composition of the catalyst feedstock, reaction products, and their relative percentages along with the catalyst structure and surface characteristics before and after testing was necessary.

To obtain information about the catalyst performance, the nature of the reaction feedstock and product mixture along with the relative percentages of the species present were determined. The necessary analyses methods and characterization processes are described below.

## **5.2 Feedstock and Product Analyses**

Equation [6] shows the catalytic dehydrogenation of 2-t-butyl-9,10-dihydroxyanthracene ( $H_2TBAQ$ ) into 2-t-butyl-9,10-anthraquinone (TBAQ). As mentioned before, some byproducts were expected to be produced during this catalytic process.

The best instrumental quantitative analytical techniques available to be used for the analyses of the feed and reaction products are nuclear magnetic resonance spectroscopy (NMR), ultraviolet-visible spectroscopy (UV/Vis), gas chromatography-mass spectrometry (GC/MS), and Fourier transform infrared spectroscopy (FTIR). From these techniques, NMR spectroscopy was the most useful for determining the presence and relative percentages of the different structurally related quinone species present in the feedstock and reaction products mixture.

The hydrogenation of TBAQ (**I**) under the reaction conditions performed in this study, see Section 2.4, led only to the production of H<sub>2</sub>TBAQ (**II**). When catalytically dehydrogenated (as in Equation [6]) at relatively high temperatures and in the presence of the metal active sites and support material (see Section 4.4), the H<sub>2</sub>TBAQ potentially could produce several side products in addition to the TBAQ (see Figure 5).

Due to their structural similarity, the IR spectra of these compounds provided no definite differentiation between the species. Neither the OH nor the aliphatic or aromatic absorption regions provided a clear resolution. Besides the

limited reliability of IR spectroscopy as a quantitative analytical technique, the high polarity of the NMP solvent made it more difficult to use this technique. The N-methyl-2-pyrrolidinone dissolved the NaCl windows of the liquid IR sample cell. And finally, the very dark color of the product mixture reduced the IR transmission.

Ultraviolet-visible spectroscopy is considered to be a powerful quantitative technique. Unfortunately, the reactants and products of the reaction (Equation [6]) had similar UV-visible spectra which made the use of UV-visible spectrometry of very limited value in distinguishing between these species in the reaction mixture.

The use of GC/MS spectroscopy was also limited by the special properties of the reaction products. The large quantity of solvent made GC/MS analysis difficult. Thermal decomposition of the sample in the injection port also produced species not related to the catalytic reactions. Nevertheless, the GC/MS data were useful and will be discussed briefly later (see Section 5.2.4). After comparing all available techniques, NMR spectroscopy was selected as the best analytical method for this study.

### 5.2.1 Results of Analyses Using the 90 MHz NMR Instrument

During the early stages of this study, a Varian 90 MHz NMR instrument was used for the analyses of the catalytic reaction products. The degree of conversion of TBAQ upon its reduction by  $H_2S$  (Equation [5]) to  $H_2TBAQ$  has been successfully followed using NMR spectroscopy. Integrated peak intensities in three regions of the NMR spectrum were used to calculate the relative percentages of the product species present. These regions were the t-butyl group protons in the range 1.3-1.6 ppm; the aromatic protons in the 7.0-9.0 ppm region; and the hydroxyl protons in the range 9.5-11.0 ppm. The TBAQ aromatic protons gave a multiplet of peaks centered at about 8.2 ppm. Upon hydrogenation, the intensity of this TBAQ multiplet decreased and two new sets of proton signals appear centered at about 7.5 and 8.5 ppm from the  $H_2TBAQ$ , see Figure 6.

The peak intensities of the two sets of  $H_2TBAQ$  multiplets increased with an increase in the mole percent of  $H_2TBAQ$  in solution. Upon dehydrogenation, the peak intensities of  $H_2TBAQ$  proton signals clearly decreased, and the corresponding TBAQ protons signal increased. By comparing the ratio of the integrated peak areas of the  $H_2TBAQ$  and TBAQ proton signals, the relative mole percent of

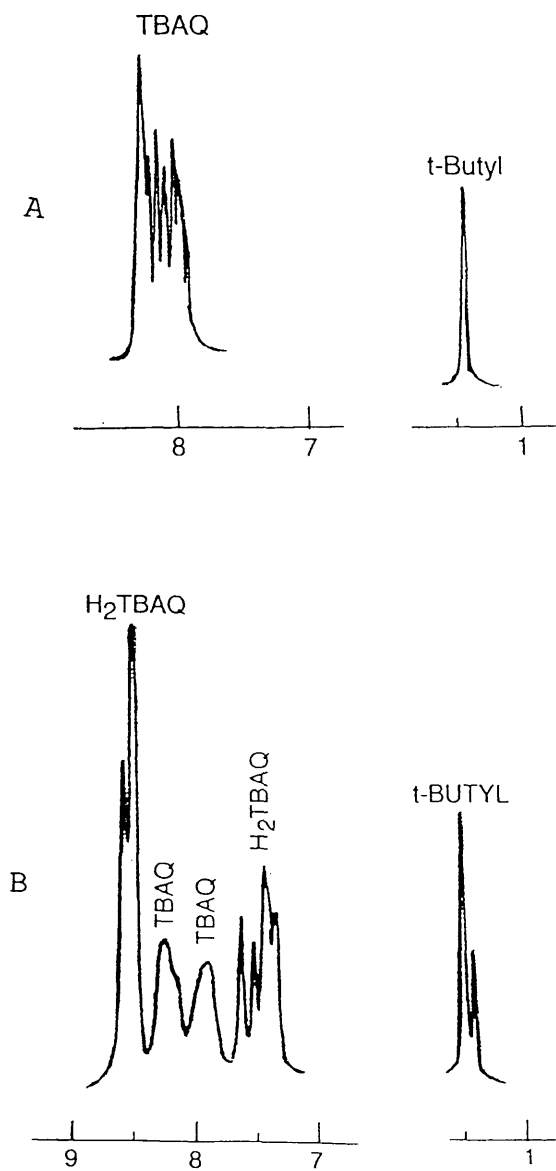


Figure 6: A sketch of NMR spectra of (A) TBAQ (B) TBAQ and H<sub>2</sub>TBAQ in NMP using the 90 MHz NMR instrument.

H<sub>2</sub>TBAQ in the feedstock or the product mixture was obtained.

In the initial phases of this research, the mole percent of H<sub>2</sub>TBAQ was determined using the integrated peak-area of the hydroxyl group. This mole percent was computed by multiplying the hydroxyl group peak intensity by a factor representing the ratio between the hydroxyl group hydrogens and the aromatic-hydrogens per molecule of H<sub>2</sub>TBAQ. There are two hydroxyl group hydrogens and seven aromatic hydrogens per molecule of H<sub>2</sub>TBAQ. Hence the factor was 3.5.

To obtain the relative mole percent of H<sub>2</sub>TBAQ in solution, the multiplication product (integrated peak area of OH group x 3.5) was then divided by the total integrated peak area of the entire aromatic region (TBAQ + H<sub>2</sub>TBAQ + etc.), see Equation [33]. Later in the study, this method of calculation proved to be incorrect because the hydroxyl-proton signal often disappeared while the signal for H<sub>2</sub>TBAQ aromatic protons remained.

$$\% \text{ moles } H_2TBAQ = \frac{3.5 ( OH \text{ peak area } )}{\sum \text{ aromatic peak area }} \quad [33]$$

Because of the early disappearance of the hydroxyl-group signal, the integrated peak area of the aromatic protons seemed better suited for the calculation of the relative mole percents of TBAQ and H<sub>2</sub>TBAQ in the solution mixture. The poor resolution and the presence of many multiplets in the aromatic signal region along with the observation of overlapping peaks in the t-butyl group region led to further defining these calculations (Figure 7). The overlapping signals were attributed to byproducts formed during the catalytic dehydrogenation reaction. In this group of compounds it was obvious, after careful investigation of the NMR spectra produced, that the t-butyl signals were more sensitive to changes in molecular structure than the aromatic region signals where overlap between the multiplets of the structurally similar species occur. Therefore, it became apparent to use the integrated peak areas of the t-butyl signals for the calculation of the relative mole percents, especially when trace amounts of byproducts are present.

Several attempts were made to follow the reaction by expanding the t-butyl group region of the spectrum. Unfortunately, this was limited because of the poor resolution of the 90 MHz NMR instrument. A 300 MHz NMR

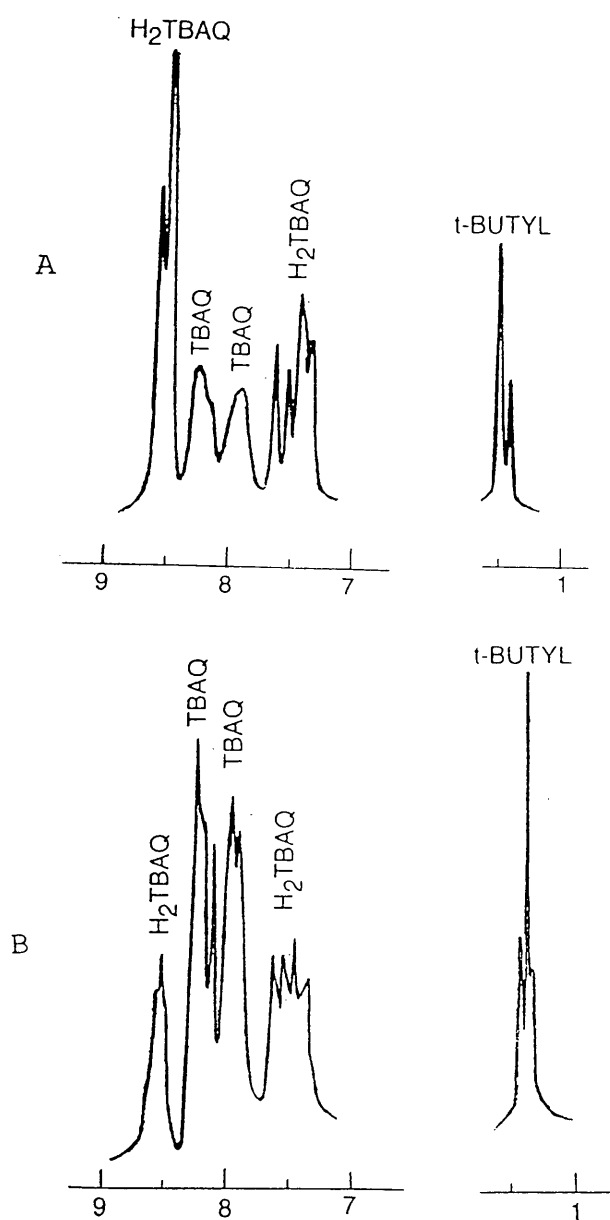


Figure 7: A sketch of NMR spectra of (A) typical catalyst feed and (B) catalytic reaction product using the 90 MHz NMR instrument.

instrument was found to provide sufficient resolution to observe individual signals of the TBAQ, H<sub>2</sub>TBAQ, and the reaction byproducts.

### 5.2.2 Results of Analyses Using the 300 MHz NMR Instrument

The well-resolved t-butyl group peaks obtained using the 300 MHz Fourier transform NMR provided an accurate method of determining the relative percentages of the catalytic reaction products (see Figure 8). The increased resolution allowed the use of the integrated t-butyl peak areas to quantify TBAQ, H<sub>2</sub>TBAQ, and the various by-products of the dehydrogenation reaction (Equation [6]).

Even with this high-resolution NMR instrument, the aromatic region showed overlap between the signals of the various quinone species which prevented their use in monitoring the reaction. Clearly, the well resolved signals in the t-butyl region gave the most accurate determination of the percentages for the various species.

These side reaction products were identified as 2-t-butyl-9-anthrone **XXII** (TBAN 1), and its isomer, 2-t-butyl-10-anthrone **XXI** (TBAN 2); the 2-t-butyl-9-hydroxyanthracene **XIX** (TBANOL 1), and its isomer, 2-t-butyl-10-

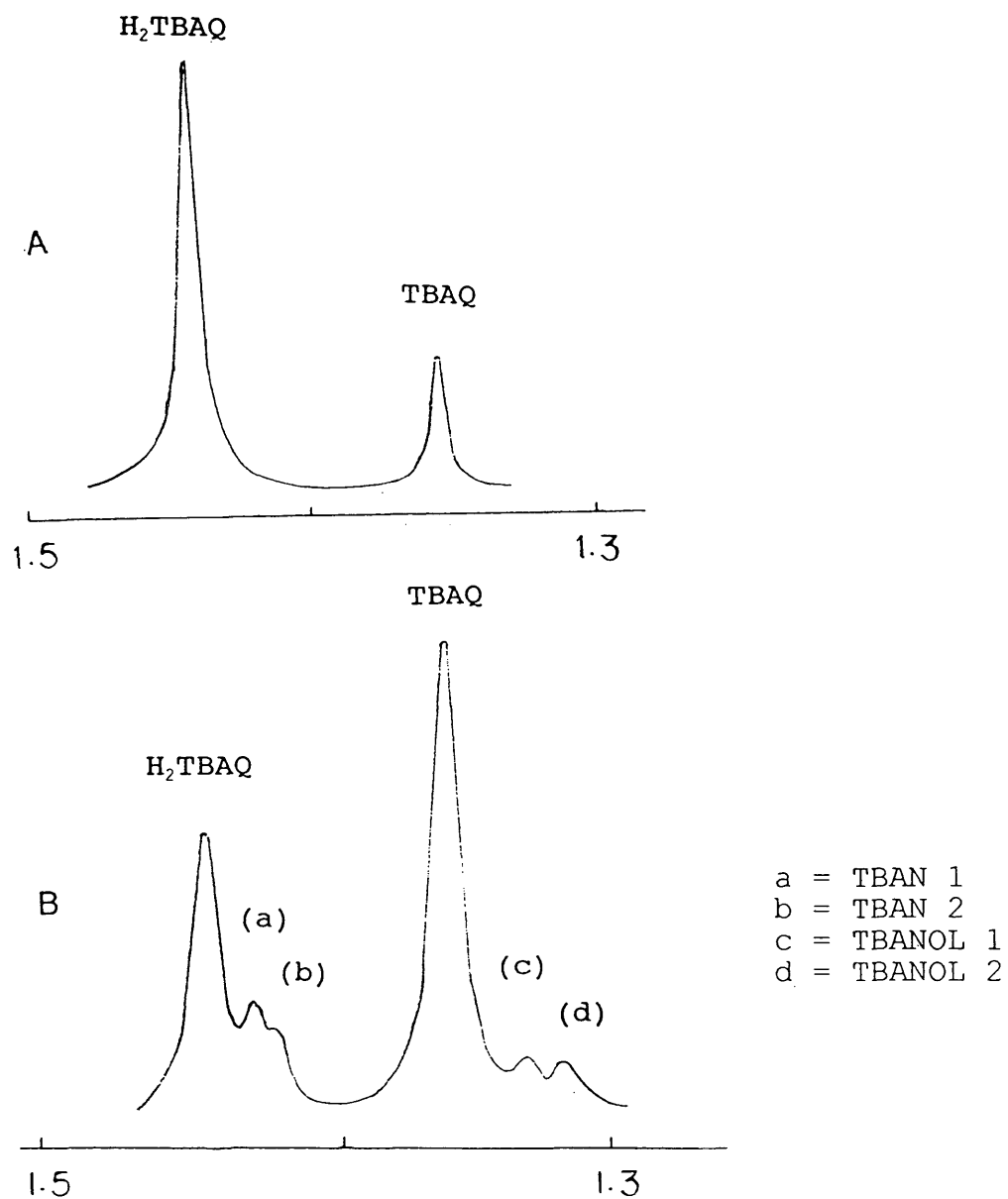


Figure 8: A sketch of signals in the t-butyl region of (A) catalyst feedstock and (B) dehydrogenation reaction product using the 300 MHz NMR instrument.

hydroxyanthracene **xx** (TBANOL 2). The structures for these compounds were shown in Figure 5.

### 5.2.3 Results of Gas Chromatographic Analyses

Gas chromatographic analyses of the gaseous products from the catalytic reaction depicted in Equation [6] showed that the major product was hydrogen gas. However, trace amounts of aliphatic hydrocarbons were also observed in some test products. These hydrocarbons were mostly methane, isomeric butanes and butenes, and isomeric pentanes and pentenes. These results indicated that the dehydrogenation reaction was taking place and the major action of the platinum catalysts tested was the dehydrogenation of H<sub>2</sub>TBAQ to TBAQ. At the same time, these results confirmed the information obtained from the NMR spectroscopic analyses about the dehydrogenation reaction and the conversion of H<sub>2</sub>TBAQ to TBAQ and hydrogen.

### 5.2.4 Results of Gas Chromatography-Mass Spectrometric Analyses

To corroborate the data obtained from the NMR spectroscopy analyses, two samples of the reaction products, obtained from a platinum catalyst, were analyzed using GC/MS. Unfortunately, the high boiling point and viscosity of the product mixtures made the analysis very difficult.

The major GC peaks obtained showed  $m/z$  values of 266 and 264 which corresponded to  $H_2$ TBAQ or its tautomers TBHOAN 1 and 2 and TBAQ, respectively. The presence of minor anthrone (TBAN) at  $m/z = 250$  and anthracene at  $m/z = 234$  were also detected. Additionally, other very low intensity GC peaks were observed. The anthracene and anthrone were likely as thermal degradation products from the two main quinones which probably occurred at the high temperature of the injector inlet and not during the catalytic reaction. The high viscosity of the samples may also have assisted the high temperature in forming these degradation products.

### 5.3 Catalyst Evaluation

As mentioned in Chapter 2, the literature showed that selected supported metal and metal oxide catalysts can be considered as potential candidates for the dehydrogenation step (Equation [6]). The principle of microscopic reversibility suggests that good hydrogenation catalysts are also good candidates for the corresponding dehydrogenation reactions (3).

Metal oxide catalysts have been employed in a variety of catalytic reactions. Supported and unsupported oxides of chromium, copper, manganese, thorium, and zinc have been

used for the catalytic dehydrogenation of aliphatic alcohols, alkanes, and alkenes. Almost all of these oxide catalysts have shown a dehydration activity toward alcohols to produce various hydrocarbons. In our studies, dehydration is undesirable and will lead to the production of anthracene; hence, a third step to re-oxidize this anthracene to TBAQ would be needed. With the possible presence of traces of sulfur and hydrogen sulfide in the feed streams, zinc and copper oxide catalysts were not good candidates for this study due to their severe susceptibility to sulfur poisoning (66).

Supported cobalt, iridium, iron, nickel, osmium, palladium, platinum, rhodium, and ruthenium metal catalysts were selected as the optimum candidates for the HYSULF process. This group of metals has been extensively used in a wide variety of hydrogenation reactions (67,68,69). While the platinum oxide has been reported to be easily deactivated, ruthenium catalysts demonstrated superior activity over palladium and platinum catalysts in the hydrogenation of saturated aliphatic aldehydes. However, palladium catalysts were the most active in the hydrogenation of aromatic aldehydes. While all three metal catalysts demonstrated high ring saturation and C-O bond

hydrogenolysis activity in the hydrogenation of aromatic ketones and diketones, rhodium catalysts showed the capability to saturate the ring without cleaving the C-O bond (67,68).

In catalytic naphtha reforming, it has been reported that supported platinum-group metal catalysts have higher activity than other catalysts. Among this group of transition metals, platinum metal has the highest reforming activity and selectivity (70). The possible presence of trace amounts of sulfur or  $H_2S$  in the catalyst feedstock, eliminated the use of nickel catalysts for this process. Nickel catalysts have been reported to be very vulnerable to sulfur poisoning and do not survive feedstocks containing more than 0.2-0.5 ppm of sulfur (66).

The successful use of the platinum-group metal catalysts in large industrial hydrogenation processes, such as the autoxidation of anthraquinone in the synthesis of  $H_2O_2$ , makes the platinum group good potential candidates to be used in this process. For this reason, platinum, palladium, rhodium and palladium-gold catalysts on different supports were prepared and tested. Discussion of the results obtained from these studies is presented in the next

section.

To determine a catalyst's activity and selectivity towards the production of hydrogen in this process, it is necessary to introduce the mathematical relations used to perform the data calculations. Catalyst activity is defined as the difference in mole percent of H<sub>2</sub>TBAQ in the catalyst feedstock and that in the reaction product divided by the mole percent of H<sub>2</sub>TBAQ in the feed (see Equation [34]).

$$\text{Catalyst Activity} = \frac{(\% H_2TBAQ_f - \% H_2TBAQ_p)}{(\% H_2TBAQ_f)} \quad [34]$$

where f represents the feed, and p represents the product.

However, the theoretical mole percent of H<sub>2</sub>TBAQ converted to TBAQ, hydrogen and other products can be calculated using Equation [35].

$$\text{Theo. Moles } H_2\text{TBAQ Convd.} = \left\{ \frac{\% \text{Mole } (H_2\text{TBAQ}_f - H_2\text{TBAQ}_p)}{100} \times \frac{\left( \frac{\text{Wt } (H_2\text{TBAQ} + \text{TBAQ})}{\text{Wt Feed}} \right) (\text{Wt of L. P. Collected})}{(\text{Molecular Weight. of } H_2\text{TBAQ})} \right\} \quad [35]$$

where:

f represents the feed.; p represents the product; Wt: weight, and L: liquid

In order to determine the actual moles of  $H_2\text{TBAQ}$  converted to hydrogen and TBAQ, one must know the moles of hydrogen produced. In order to perform this calculation, the volume of hydrogen produced is corrected to the atmospheric pressure, room temperature, vapor pressure of water, pressure inside the collection buret, and so on.

After determining the actual moles of  $H_2\text{TBAQ}$  converted (equals the actual number of moles of hydrogen produced) and the theoretical moles of  $H_2\text{TBAQ}$  reacted, one can calculate the catalyst selectivity towards hydrogen (Equation [36]).

$$\%H_2 \text{ Selectivity} = \frac{N_{H_2}}{\text{Theo. Moles } H_2\text{TBAQ Conv.}} \times 100\% \quad [36]$$

### 5.3.1 Supported Metal Oxide Catalysts

Chromium oxide on alumina ( $\text{Cr}_2\text{O}_3/\text{Al}_2\text{O}_3$ ) catalyst has been extensively used in naphtha reforming (70). It is known that this catalyst has some tolerance to sulfur poisoning. These two factors stimulated the testing of this catalyst as a possible candidate for this study.

A commercial chromia/alumina catalyst (Strem Chemicals) was evaluated for the dehydrogenation of  $\text{H}_2\text{TBAQ}$  (see Section 3.1 in Chapter 4). At the beginning, the catalyst was tested using a 1/2" quartz tube catalytic reactor working under atmospheric pressure for that day in Golden, Colorado. No hydrogen was collected from these tests. Later, the catalyst was tested using the 1/2" stainless steel reactor at different reaction conditions such as back pressure, temperatures, and flow rates. No hydrogen was collected in any test and a proton signal that corresponds to anthrone was present in the NMR spectrum.

### 5.3.2 Supported Metal Catalysts

From the platinum group metals, supported catalysts of platinum, palladium, rhodium, and a bimetallic palladium-gold were prepared (see Section 4.3) and evaluated at different reaction conditions. A platinum on lanthana

( $\text{La}_2\text{O}_3$ ) modified alumina catalyst was also tested and a palladium-gold on lanthana modified quartz catalyst was also prepared and tested. Finally, a rhodium on lanthana modified silica grade 3 catalyst was prepared and evaluated.

#### **A. Effect of Support Type on Catalyst Performance**

A catalyst support has been shown to play a major role on the catalyst performance. Changing the support material or additives (dopants or modifiers) causes a significant change on the catalyst activity and selectivity (71). At low temperatures, the most widely used catalyst supports are alumina and silica of various specific surface areas, pore sizes, and pore-size distributions (72).

A high surface area oxide exposes centers that have either acidic or basic characteristics depending on the its cation or central atom properties. While oxides of alkaline earth metals are known to have basic properties, alumina is amphoteric, and silica-alumina and zeolites are acidic. These centers can be protic (Brønsted) or aprotic (Lewis) in their acid-base behavior (70,72). Although alumina shows no Brønsted acidity, it exhibits Lewis acidity after calcination at relatively high temperatures. This is due to the removal of an OH group during the calcination leaving an

exposed aluminum cation capable of accepting a pair of electrons (3). Silica on the other hand, shows neither Brønsted nor Lewis acidity (73).

The anthrone production from the chromium oxide on alumina catalyst tests is attributed to the acidic properties of alumina. This behavior of the support material decreases the catalyst selectivity by assisting the production of the undesired anthrone. Therefore, for a catalyst support to be promising, its acidity must be lowered or, if possible, eliminated.

As mentioned in Chapter 4 (Section 4.3.1.A), basic oxides of lanthanide metals such as Ce and La can be used to neutralize the surface acidic sites of the support (see Figure 9). These dopants, also, enhance the dispersion of the metal crystallites on the support surface which results in an increase in the catalyst surface area and consequently catalyst activity (61). Among the commonly used catalyst supports, alumina is known to have the most acidic properties (73).

In general, alumina-supported catalysts showed an acceptable activity, but have low hydrogen selectivity when

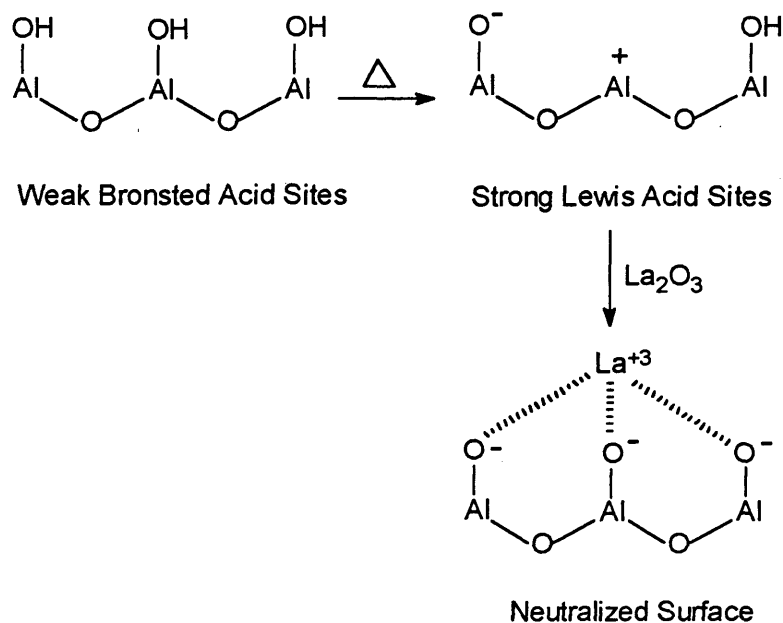


Figure 9: Neutralization of the support acidic sites by the dopant material.

compared to silica supported catalysts. This low selectivity is due to the production of TBANOL 1 (**XIX**) and its isomer TBANOL 2 (**XX**) as well as TBAN 1 (**XXI**) and its isomer TBAN 2 (**XXII**) byproducts which consumed the hydrogen that was supposed to be produced according to the reaction presented in Figure 10. The acidic support definitely enhanced the production of byproducts and two moles of hydrogen, which is supposed to be produced, were lost for every mole of byproducts produced (see Figure 10). One mole of hydrogen was used in the production of a mole of water.

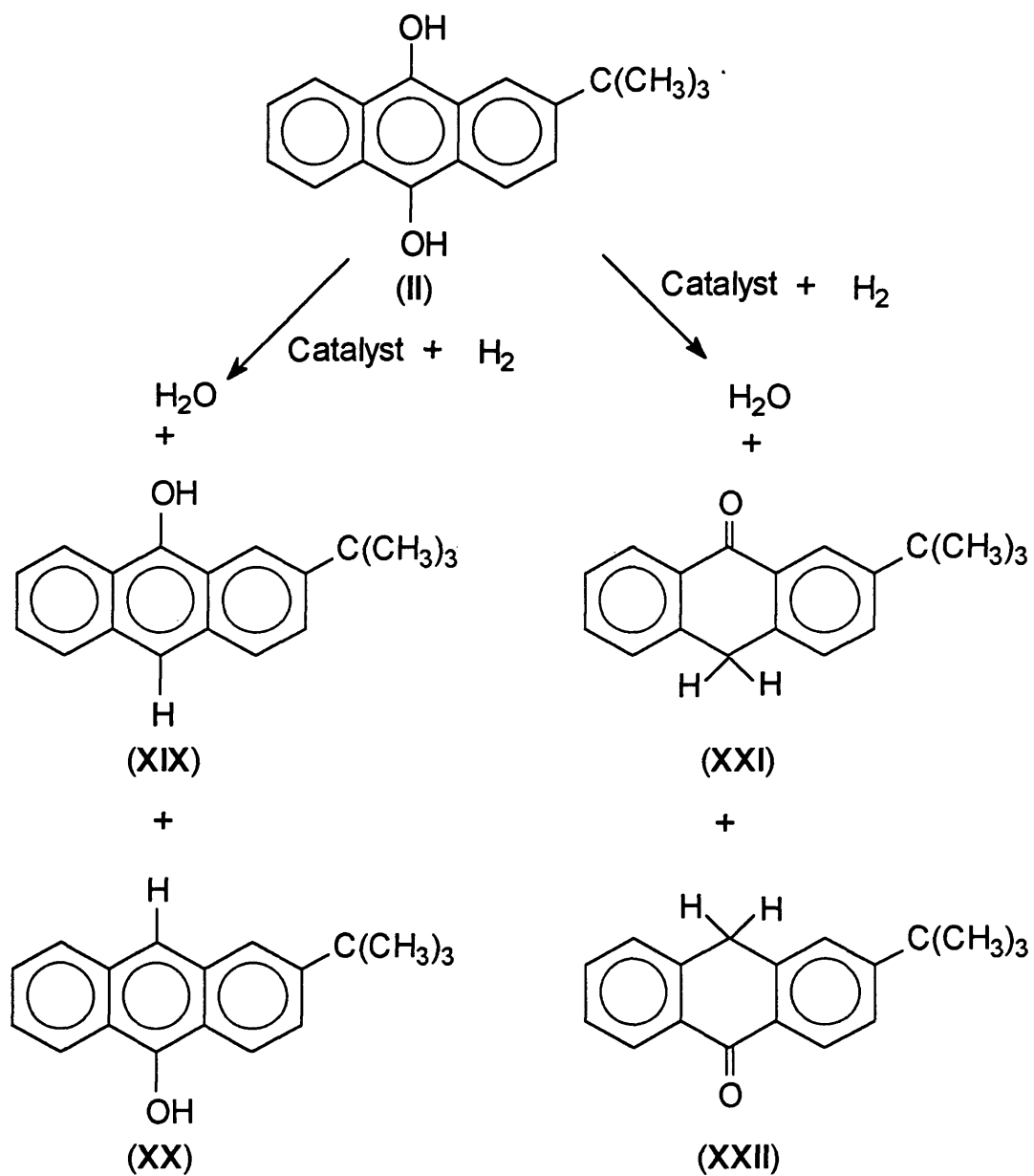


Figure 10: Production of byproducts in the presence of an acidic catalyst.

The second mole was either used in ring saturation to produce TBAN 1 (**XXI**) or its isomer TBAN 2 (**XXII**), or remained as a hydroxyl hydrogen (one atom) and an aromatic hydrogen (the second hydrogen) to produce TBANOL 1 (**XIX**) or its isomer TBANOL 2 (**XX**). However, another possible way of consuming the two moles of hydrogen is the production of two moles of the TBAN isomers (1 and 2) or two moles of the TBANOL isomers (1 and 2). The poor resolution of the 90 MHz NMR instrument did not allow the determination of the byproducts percentages.

The neutralization effect of  $\text{La}_2\text{O}_3$ , in reducing the alumina support acidity, was clear from the results obtained from the platinum on lanthana doped alumina ( $\text{Pt}/\text{La}_2\text{O}_3/\text{Al}_2\text{O}_3$ ) catalyst test. Even though both catalysts were similar in terms of activity, the lanthana doped catalyst had higher hydrogen selectivities when compared to the undoped Cyanamid Aeroform<sup>R</sup> ( $\text{Pt}/\text{Al}_2\text{O}_3$ ) catalyst. It was found, in this study, that the metal loading did not significantly affect the catalyst performance. Therefore, it was reasonable to compare the efficiency of these two platinum on alumina catalysts.

On the other hand, silica is known to be more neutral than alumina. This was obvious when comparing the results obtained from silica supported platinum catalysts with those obtained from alumina supported platinum catalysts. In general, the platinum on doped silica catalysts were lower in activity compared to those supported on lanthana doped alumina. However, the platinum on doped silica catalysts had higher hydrogen selectivities than those of platinum on lanthana doped alumina support.

It is worth mentioning that this same behavior was observed in the comparing the platinum metal catalysts supported on the more acidic grade 3 silica with those supported on the less acidic silica grade 57. Catalysts on lanthana doped silica grade 3 were higher in activity, but lower in hydrogen selectivity than their analogues which were supported on lanthana doped silica grade 57.

Results obtained using the acidic supports directed the research toward the use of the totally basic magnesium oxide (MgO) as support material. Platinum supported on magnesia (Pt/MgO) catalyst showed a higher activity than the lanthana doped silica 57 platinum (Pt/La<sub>2</sub>O<sub>3</sub>/SiO<sub>2</sub>) catalyst. However, in terms of hydrogen selectivity, the Pt/MgO

catalyst was significantly less than the Pt/La<sub>2</sub>O<sub>3</sub>/SiO<sub>2</sub> (silica 57) catalyst. This low selectivity can be attributed to the presence of the highly basic OH groups on the MgO surface. The OH group will abstract a hydrogen, as an H<sup>+</sup> ion, from the H<sub>2</sub>TBAQ to form water and HTBAQ<sup>-</sup> anion. In the presence of surrounding hydrogen this anion can easily lose an OH<sup>-</sup> to form TBAN, see Figure 11.

The combination of the above surface studies indicated that neither highly acidic nor highly basic supports are proper for the dehydrogenation reaction. This conclusion led to the use of the more neutral quartz as a catalyst support. However, the low surface area of quartz resulted in low dispersion of the metal on the surface. To increase the metal dispersion, quartz was doped with lanthanum oxide before the impregnation of the metal. The doped quartz catalysts had very good activities, but low hydrogen selectivities when compared to silica supported

These observations indicated that the hydrogenolysis activity is mainly a metal function on the low acidity supports (for this behavior see refs. 29,30,31). However, on the high acidity supports both the metal and the support platinum catalysts material have hydrogenolysis functions.

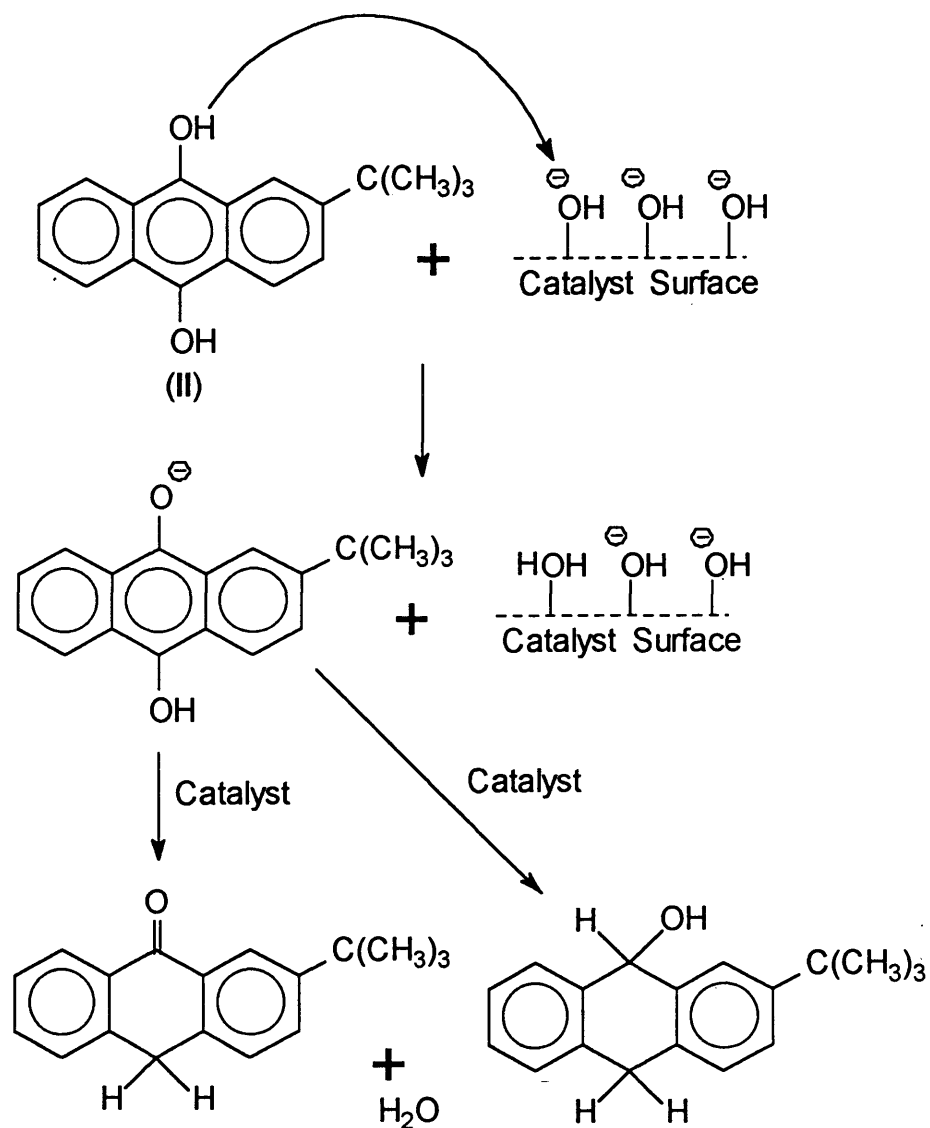


Figure 11: Effect of basic support material on byproducts production in the catalytic dehydrogenation of H<sub>2</sub>TBAQ.

In conclusion, the best catalyst support to be used in the dehydrogenation process was lanthana doped silica 57, and the worst was alumina with undoped silica 57 with lanthana doped quartz in between.

### **B. Effect of Metal Type on Catalyst Performance**

Available literature showed that supported palladium, platinum, and rhodium catalysts performed well for the hydrogenation of quinones to hydroquinones (24,25,26,27). Supported catalysts of these three metals were tested as candidate catalysts for the dehydrogenation of H<sub>2</sub>TBAQ. The palladium and rhodium catalysts, did not perform well in the dehydrogenation reaction, Equation [6]. Platinum catalysts showed the best dehydrogenation activities of H<sub>2</sub>TBAQ at all reaction conditions and on all catalyst supports tested (see Chapter 4). Selectivities of >60% were obtained and the catalysts survived even in the presence of coking or poisoning materials. These catalysts also remained active and selective independent of the time of the test. At the end of most of the tests, the catalysts showed better hydrogen selectivity than at the beginning. This could be due to poisoning or deactivation of the very highly active sites which are responsible for the hydrogenolysis function of the catalyst.

### **C. Effect of Metal Concentration on Catalyst Performance**

Changes in metal concentration or loading can affect the catalyst performance by changing the number of metal active sites, or degree of dispersion, on the catalyst surface. Metal dispersion is defined as the ratio of the number of surface metal atoms to the total number of metal atoms in the catalyst. A dispersion of one unit means that all the metal atoms are exposed to the reactants. Due to the increase in the number of atoms in the bulk compared to that on the surface, the fraction of metal atoms exposed decreases with increasing particle size (66).

However, the literature shows that the use of the impregnation technique in catalyst preparation results in the dispersion of the metal as small crystallites on the support surface. When there is no specific chemical interaction between the metal salt and the support material, the structure of the support determines the metal crystallite size. This was the case when silica was impregnated by the platinum salts. When using the impregnation method, one can change the metal loading by changing the concentration of the metal salt in solution. It was reported (70) that using a high surface area silica with platinum loadings up to 5% caused the catalyst surface

area to increase linearly with increased metal loading. Within this linear range, the number of crystallites increased and the average crystallite size remained unchanged. Above the 5% loading, the surface area increased more gradually and the average Pt crystallite size increased while the number of crystallites remained constant. On the other hand, alumina is known to have a lower surface area than silica. Therefore, when same loadings of platinum were impregnated on alumina, larger crystallites sizes were obtained (70).

In this study, the effect of metal loading on the catalyst performance was tested on the Pt/quartz catalysts. Catalysts with 0.50%Pt and 2.75%Pt loadings on lanthana doped quartz were prepared and tested for the dehydrogenation of H<sub>2</sub>TBAQ. The two catalysts showed very comparable activities and slightly different hydrogen selectivities. The lower loaded catalyst had the lower hydrogen selectivity. These results indicated that the presence of the La<sub>2</sub>O<sub>3</sub> dopant led to a uniform dispersion in both cases, but larger crystallite were formed in the case of the higher loading (2.75%Pt).

#### D. Effect of Pressure on Catalyst Performance

It has been reported that pressure has a crucial effect on the reaction selectivity in the catalytic hydrogenation of organic compounds (68). In this study, the reaction pressure was controlled by means of a Mity-Mite back pressure regulator, see Section 4.4. For the following reasons, controlling the reaction pressure was very important:

1. To prevent the evaporation of the NMP solvent. This is very crucial to avoid severe coking of the catalyst by the aromatic anthraquinones.
2. In order to avoid the hydrogenolysis of the C-O bond, the reaction pressure should be at a determined level. Because at very high back pressures, produced hydrogen will remain in the catalyst vicinity thus providing a higher chance for the hydrogenolysis reaction to take place.

Allowing the hydrogen gas to leave the reaction vessel will also avert any kind of reaction equilibrium from occurring. If an equilibrium is attained, in the reaction vessel, both hydrogen selectivity and the catalyst activity will be lower.

The effect of pressure on the catalyst activity and selectivity for the dehydrogenation of  $H_2TBAQ$ , Equation [6], was studied. Results obtained showed that the optimum pressure was just high enough to avoid evaporation of the NMP at any temperature. Therefore, at all reaction temperatures, the pressure had to be raised or lowered to prevent the evaporation of NMP and minimize the quantity of hydrogen present in the catalyst vicinity.

#### **E. Effect of Temperature on Catalyst Performance**

In catalysis, the reaction temperature can highly influence the catalyst performance. For each catalytic reaction, there is an optimal operating temperature range where the catalyst shows the best performance (74, and references therein). The activation energy of the interaction between the catalyst surface active sites and the reactants or products plays a major role in determining the reaction pathways. For this reason, a catalyst can be active and selective at a certain temperature or neither, both, or one at a different temperature depending on the nature of their interaction and the kind of surface bond formations involved (63).

To determine the optimum thermal catalytic conditions for the dehydrogenation of H<sub>2</sub>TBAQ, catalyst candidates were tested at temperatures range of 200-290°C. Each catalyst demonstrated optimum performance in a unique temperature range. The optimal temperature range for the platinum on doped silica 57 catalysts was 260-280°C.

#### **F. Effect of Residence Time on Catalyst Performance**

Residence (contact) time is defined as the time that the feedstock spends in the vicinity of the catalyst. Mathematically, its the volume of the catalyst bed (cm<sup>3</sup>) divided by the volumetric flow rate of the catalyst feed (cm<sup>3</sup>/minute). Space velocity, a more commonly used term, is the reciprocal of the residence time (66).

In this study, the effect of the residence time on the catalyst's activities and selectivities showed that the more time the reactants spend close to the catalyst the greater the catalyst efficiency. However, if the catalyst has an undesirable function, like hydrogenolysis, it also will become more pronounced with increasing residence time. Because the metal catalysts tested have a hydrogenolysis tendency, moderate residence times were found to be optimum. Unless the highly active metal sites underwent changes, like

being coked, the shorter residence times provided greater selectivities. However, with very small particle size catalysts, the film diffusion of the feed directly controlled the residence time. Hence, at high space velocities, the catalyst showed low activities and selectivities. In conclusion, one can summarize that for every particle size, there are optimum residence times for the catalyst to be active and selective.

#### **G. Effect of Particle Size on Catalyst Performance**

The catalyst performance can be significantly affected by the particle size of the catalyst. It has been reported that the hydrogenation rate of nitrobenzene in acetic acid using a platinum on carbon catalyst was highly dependent on the support particle size (75). In another study, the effect of particle size on the catalytic properties of rhodium on silica or alumina was investigated. The researchers found that changes in the catalyst particle size caused changes in the catalyst activity or selectivity (71).

In the present study, the particle size effect on the catalyst performance for the dehydrogenation of H<sub>2</sub>TBAQ to hydrogen and TBAQ was investigated. The results for the reaction conditions used indicated that the best particle

size for the Pt/La<sub>2</sub>O<sub>3</sub>/SiO<sub>2</sub> grade 57 was the middle size, i.e. 0.70-0.42 mm.

The behavior of the larger and smaller sizes can be explained as follows: For the larger particle size, pore diffusion played a major role. Hence, the reactants would stay inside the pores for longer times, thus allowing more byproducts to be produced. In the case of the smaller particle size, the film diffusion played a significant role. Therefore, the reactants would remain in contact with the catalyst surface for longer times and, hence, more side reactions would occur.

#### **H. Effect of Poisons and Coke Precursors on Catalyst Performance**

Poisons can be categorized into two different groups, permanent and temporary poisons. In the case of permanent poisons, the catalyst properties are difficult to restore and drastic treatment to remove the poison is required. This often destroys the catalyst structure. In contrast, with temporary poisons, the catalyst regains its original properties as soon as the poisoning material is removed from the reaction mixture (76).

Permanent poisoning typically result from the strong chemisorption (bond formation) of the poisoning material on the metal surface. In some catalytic reactions, poisons are introduced on purpose to remove the very active metal sites that would produce undesired products. Elements of groups VB (N, P, As, Sb) and VIB (O, S, Se, Te), or molecules containing these elements, can be strong catalyst poisons. Due to the great stability of the metal sulfides, sulfur is the most prominent poison. The equilibrium position of the reaction, Equation [37], is far to the right for most metals (66,70). Using magnetic susceptibility measurements, Dilke *et al.* have shown that electrons from methyl sulfide enter the *d* band of the metal to form a strong coordinative link upon adsorption (77).



Coke formation, or carbonaceous deposit, can also alter the catalyst performance. The formation of a small carbonaceous residue may cause partial poisoning of the catalyst surface, thereby blocking some surface sites resulting in a more selective catalyst (66).

In this study, the hydrogenolysis reactions caused by the presence of adatoms which are highly reactive are undesired (see Figure 12). Coking or poisoning these active metal surface sites (adatoms) reduces the hydrogenolysis, hence, increases the catalyst selectivity. To accomplish this purpose, methyl sulfide (a poisoning material) was added to the feed of a platinum on silica (grade 57) catalyst during testing. The effect of cyclopentene, a coke precursor, on a Pt/SiO<sub>2</sub> (grade 57) was also investigated. Neither test affected the catalyst performance. This indicated that the metal surface was already poisoned by the trace amounts of sulfur or H<sub>2</sub>S present in the feedstock. The observation of a black layer on the copper gaskets used to seal the steel catalytic reactor parts together, accompanied by the results obtained initiated the need to analyze one of the gaskets. An electron microscopic analyses of the gaskets surface showed that the black layer was cuprous sulfide, Cu<sub>2</sub>S. This confirmed the presence of traces of sulfur in the catalyst feed which in turn proved the assumption of the catalyst prepoisoning.

#### **I. Effect of Water on Catalyst Performance**

In the hydrogenation of aromatic compounds, the presence of water in the catalyst feed has been shown to

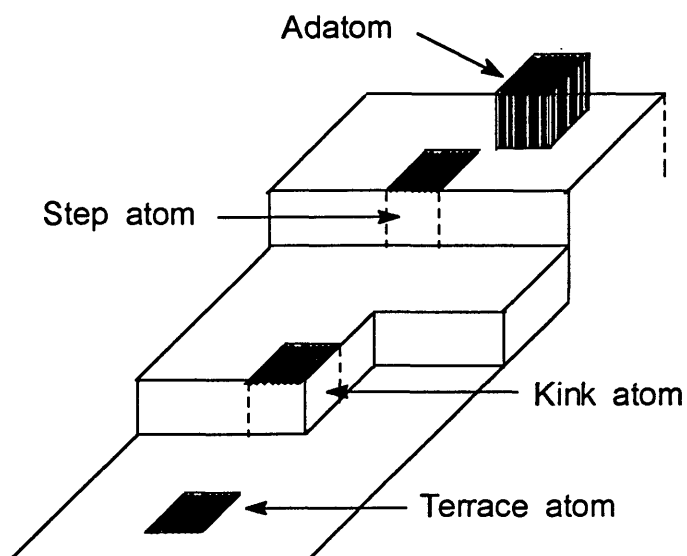


Figure 12: A hypothetical diagram of a heterogeneous catalyst surface.

have a promoting effect on the catalyst performance. Researchers found that the hydrogenation rate of aromatic compounds over carbon-supported ruthenium, palladium, and platinum catalysts increased with the presence of water in the catalyst feed (67).

In this study, the addition of water to the platinum on doped quartz catalyst feed was shown to positively affect the catalyst performance. Addition of 1 mole of water per mole of TBAQ and  $H_2$ TBAQ in the catalyst feed resulted in an

increase in the catalyst selectivity without affecting the activity. Increasing the mole ratio of added water to 2 moles ( $H_2O:TBAQ$  and  $H_2TBAQ$ ) caused a lowering of the catalyst selectivity. This increase in selectivity could be due to temporary blocking (poisoning) of the highly active catalyst sites responsible for the hydrogenolysis reactions, hence, reducing this detrimental activity.

#### **5.4 Catalyst Hydrogenation Activity**

As mentioned earlier, the principle of microscopic reversibility states that a catalyst that has a hydrogenation activity should have an activity for the reverse reaction, dehydrogenation, and *vice versa*. A test was performed to check the validity of this principle. A fresh catalyst bed was fed with a mixture of hydrogen gas and a 25% weight solution of TBAQ in NMP. The flow rate of hydrogen gas was varied with a constant flow rate of TBAQ solution. The reaction pressure and temperature were maintained at selected values while the residence time was varied.

Analysis by NMR spectroscopy showed that at the optimum residence times, a 100% conversion of TBAQ to  $H_2TBAQ$  could be obtained with no byproducts. At a higher residence

time, the byproducts (TBANOLs **XIX** and **XX**, and TBANs **XXI** and **XXII**) were detected and their mole percents increased with increasing residence times. Besides confirming that this system obeys the principle of microscopic reversibility, it was demonstrated that the catalyst has a hydrogenolysis activity even during the hydrogenation process of TBAQ (**I**).

### **5.5 Surface Analyses**

The surface of each tested catalyst was studied before and after testing. This type of measurement leads to the understanding of changes in the catalyst structure during the reaction. Hence, the change in catalyst behavior can be understood too. Changes in the surface can be as drastic as changes in crystallite size, dispersion, and catalyst composition. Poisoning and coke formation can cause different effects on the catalyst performance. These effects can range from lowering to totally destroying the catalyst activity, and/or increasing the catalyst selectivity or even changing the reaction pathway. In this study, some of the tested catalysts were analyzed by different surface analysis methods.

### 5.5.1 Surface Analyses by X-ray Diffraction

As mentioned earlier in this chapter, the catalyst activity is directly related to the percent of exposed metal on the catalyst surface. In order to have a high surface metal to total metal ratio and lower the cost of the catalyst, the metal crystallites are made as small as possible. If, for any reason, the metal crystallites agglomerate during the pretreatment or catalyst testing, a significant increase in the crystallite size occurs. This increase in size leads to a decrease in the metal surface area and hence decreases the catalyst activity.

Even though x-ray diffraction (XRD) is a bulk technique, it can provide valuable information about the crystallite size in a catalyst. Using XRD data, the average crystallite size can be calculated. This is done by comparing the XRD peak widths of the dispersed metal with that of the bulk metal. A discussion of the theory and method of particle size determination using XRD data was reported by Klug and Alexander (78).

x-Ray diffraction data provides an effective method of detecting crystallite sintering or fragmentation which may cause catalyst deactivation. An increase in crystallite

size is accompanied by narrowing the metal reflection signal. The platinum (111) peak was used to calculate the average platinum crystallite size.

Modified platinum catalysts showed wider XRD peaks compared to the unmodified catalysts, thus showing that the average metal crystallite size in the modified catalysts was smaller than that in the unmodified. These results were consistent with the purpose of using the dopant materials. The more dispersed the metal, on the support, the smaller the crystallite size will be.

Equation [38] was used to perform the peak width calculations.

$$d = \frac{57.3 k \lambda}{\beta \cos \theta} \quad [38]$$

where,  $k$  is a constant = 0.9,  $\lambda$  (wavelength of the  $\text{Cu}_\alpha$  radiation) = 1.541 Å, 57.3 = a conversion factor to convert degrees to radians,  $\theta$  = the angle of reflection, and  $\beta = (B^2 - b^2)^{1/2}$ ; where  $b$  = the width at half height for the bulk standard (metal), and  $B$  = the width at half height for the sample (78).

When compared with that of the fresh catalyst, x-ray diffraction measurements of the tested palladium on  $\text{La}_2\text{O}_3/\text{SiO}_2$  catalysts showed no significant intensity of the Pd (111) peak. This drastic decrease of the Pd (111) peak intensity of the tested catalyst explains the sudden decrease in catalyst activity at temperatures above  $260^\circ\text{C}$ . A similar observation was reported by Stachurski and coworkers in the catalytic hydrogenation of acetylene using a silica-supported palladium catalyst. The authors suggested that the migration of carbon into the palladium lattice and the formation of a carbon palladium solution is responsible for this observation (79).

Since carbon deposits form at high rather than low reaction temperatures, the decrease in the palladium peak intensity in this study could not be due to the formation of a carbon palladium solution. Two possible factors can be used to explain the disappearance of the palladium peak in this research. 1) The presence of trace amounts of sulfur in the catalyst feed may lead to the formation of a palladium sulfide. These palladium sulfide crystallites will be of small size and more dispersed on the surface. Therefore, a drastic decrease in peak intensity (or disappearance) will occur. 2) The migration of the dopant

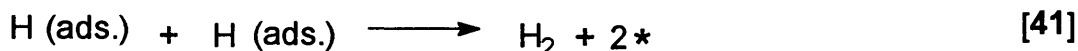
(La<sub>2</sub>O<sub>3</sub>) to the metal crystallite surface will lead to a change in the crystallite structure and a decrease in peak intensity. On the other hand, when compared with the fresh catalysts, no significant changes in the x-ray diffraction peaks of the tested platinum catalyst were observed.

### **5.5.2 Thermal Gravimetric Analyses (TG/DTA)**

TG/DTA was used to determine the amount of carbonaceous deposit on the tested catalysts. Catalysts supported on the low surface area supports, quartz and MgO, exhibited a lower weight loss (during the TG/DTA analysis) compared to the high surface area silica support. This can be attributed to the difference in porosity between supports. During the reduction of the tested catalysts, at >400°C, a yellow colored material condensed on the walls of the sample tube of the surface area determination instrument. It became clear that this yellow material was TBAQ trapped in the support pores. Several unsuccessful attempts were made to remove this residue by soaking and washing the tested catalysts with acetone and drying under vacuum at 200°C. These observations indicated that the use of TG/DTA analysis was not useful for the determination of carbonaceous deposit on the catalyst surface.

### 5.5 Proposed Dehydrogenation Mechanism

Figure 13 shows a scheme of the possible reaction pathways taking place during the H<sub>2</sub>TBAQ catalytic dehydrogenation reaction. A speculation of the possible mechanism is presented in Equations [39] through [42]. On the catalyst surface, an H<sub>2</sub>TBAQ molecule can be heterolytically adsorbed on the dehydrogenation active sites of the catalyst surface (see Equation [39]). The adsorbed HTBAQ species are postulated to undergo further heterolytic cleavage to produce another adsorbed hydrogen atom and an adsorbed TBAQ molecule (see Equation [40]). Two neighboring adsorbed hydrogen atoms then interact and are desorbed as a hydrogen molecule (see Equation [41]). The adsorbed TBAQ molecule will finally be desorbed (see Equation [42]). Figure 14 illustrates the possible surface interactions taking place during the dehydrogenation process.



where \* represents a metal active site.

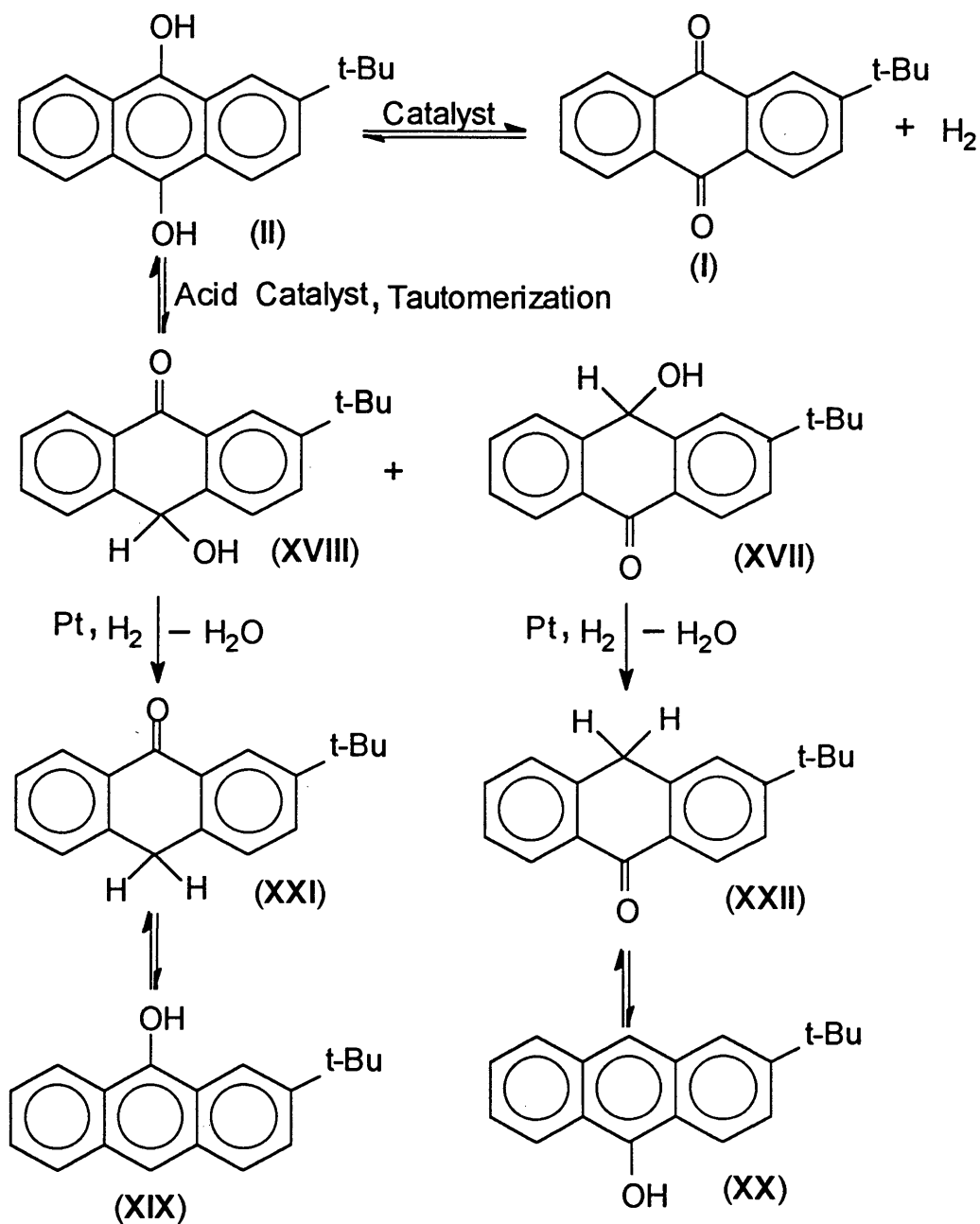
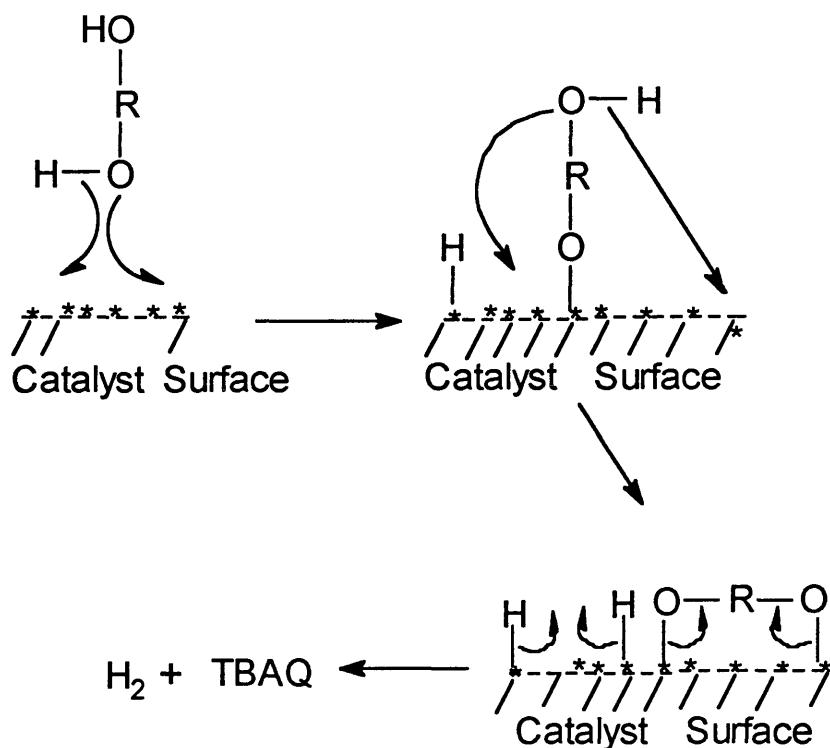


Figure 13: Possible pathways for reactions occurring during the catalytic reaction.



(R represents the hydrocarbon (or aromatic) part of the quinone molecule)

Figure 14: An illustration of the dehydrogenation reaction on the catalyst surface.

## 5.6 CONCLUSIONS

Support acidity or basicity was shown to have a major influence on the catalyst performance in the dehydrogenation of  $H_2TBAQ$ . In order for a catalyst to perform well, in terms of hydrogen selectivity, the support material had to

be neutral and of a relatively high surface area. Highly acidic supports such as alumina or highly basic supports such as magnesium oxide had significant effects on the catalyst selectivity towards hydrogen. These effects were obvious from the increase in mole percents of the byproducts as determined by NMR spectroscopy (see Section 5.3.2. A). Use of the relatively high acidic silica grade 3 also increased the formation of these byproducts compared to the low acidic silica grade 57.

Modifying the support acidity by using basic lanthanum oxide enhanced the dispersion of the metal on the support and increased the catalyst hydrogen selectivity. The use of the neutral quartz support did not show any significant increase in the hydrogen selectivity. This could be due to its low surface area.

Overall, the results showed that the best support material for this study was the lanthana-doped silica grade 57. The formation of the undesired byproducts, TBAN and TBANOL, was a result of a combination of the metal, reaction conditions, and support functionalities.

Chromium oxide catalyst,  $\text{Cr}_2\text{O}_3/\text{Al}_2\text{O}_3$  showed very low hydrogen selectivity. This low selectivity was due to the

metal oxide's tendency to dehydrate alcohols. Since, hydroquinones are structurally similar to diols, they can undergo dehydration rather than dehydrogenation by metal oxides.

Among the three platinum group metals Rh, Pd, and Pt used to catalyze the dehydrogenation of H<sub>2</sub>TBAQ, platinum was the best. Hydrogen selectivity of the rhodium and palladium catalysts on silica grade 3 was very low when compared to the platinum catalyst. Platinum catalysts on silica grade 57 gave the best hydrogen selectivities and very good activities. These catalysts survived throughout the whole dehydrogenation tests and remained active and selective. Their XRD measurements showed that the catalyst structure was not significantly changed after being tested at the various reaction conditions. Differences in metal loadings did not affect the catalyst performance. Therefore, low metal loadings can be used which will lower the net cost of the process.

Compared to other catalyst particle sizes tested, the 0.70-0.42 mm size gave the best hydrogen selectivities. It seems that this size eliminates the pore diffusion problems through the catalyst bed, hence reducing the production of

byproducts. In terms of reaction conditions, the best reaction pressure used was that just above the vapor pressure of NMP, at any reaction temperature, to prevent its evaporation. Control of the residence times also helped in avoiding film diffusion problems and hence, minimized the production of byproducts. Also, the addition of poisoning materials or coke precursors did affect the catalyst performance.

In conclusion, all platinum catalysts which were supported on lanthana doped silica grade 57 were shown to have better hydrogen selectivities when compared to the other metal catalysts evaluated in this study. The 2.75%Pt/2.50%La<sub>2</sub>O<sub>3</sub>/SiO<sub>2</sub> (grade 57) catalyst with an average particle size of 0.70-0.42 mm was the best among the platinum catalysts evaluated in this project.

Finally, from the results obtained through this study and in comparison with the viable commercial desulfurization processes, the HYSULF<sup>SM</sup> process seems to be a success. Overall, the process could be feasible for the conversion of hydrogen sulfide into hydrogen and sulfur under mild reaction conditions. Unfortunately, the formation of the byproducts and the mechanism by which they form have not

been totally determined during the duration of this project. On a more positive note, these byproducts can easily be either recycled to  $H_2TBAQ$  by  $H_2S$  or oxidized by air to produce TBAQ. Therefore, the process was, in general, a success in terms of the recovery of hydrogen from hydrogen sulfide.

## CHAPTER 6

### SUGGESTIONS FOR FUTURE WORK

This project has established new approaches and has also generated new questions concerning the conversion of  $H_2S$  into hydrogen and sulfur. Understanding the production of byproducts and how to eliminate them stands as the first priority for further research. Minimizing, or if possible, eliminating the production of these byproducts will for sure enhance the hydrogen selectivity. A careful and thorough study of the effects of variations in feed contents, catalyst conditioning, preparation, and type should lead to a better understanding of the reaction pathway by which these byproducts are formed.

The testing of other potential platinum group metal catalysts such as iridium, osmium and ruthenium is highly recommended. Catalysts of these metals have been shown to have good activities and selectivities in the redox reactions of quinones. Among these metals, ruthenium and bimetallic catalysts such as platinum-palladium, platinum-iridium, and other possible combinations of group VIII metal

catalysts have demonstrated low hydrogenolysis activities in the prementioned redox reaction. The literature shows that bimetallic catalysts have superior properties over a single metal catalyst (36). The use of a second metal can alter the negative performance of a single metal catalyst. Therefore, it is worth trying to use mixed metal catalysts such as platinum-palladium, -iridium, or -ruthenium along with other possible combinations of transition metals that have been shown to enhance catalyst properties.

In this study, differences between catalyst supports were shown to play a major role on the activity and selectivity. Preparation of new catalysts on neutral or very low acidic, high surface area supports could result in an increase in catalyst activity and selectivity. Furthermore, the use of high basic metal oxides like BaO and CeO as dopants to modify the support acidity is highly recommended.

Available literature has shown that the catalyst preparation conditions can play a major role on performance. This results from alterations in the metal dispersion and crystallite size (71). Therefore, studying the calcination temperatures and pretreatment on the catalyst activity and

selectivity is also a priority. The fact that NMP is a viscous solvent (and since pore diffusion affects the catalyst performance), the use of less viscous solvents may eliminate pore diffusion and its contribution to the formation of byproducts.

The use of pure metal screens, such as platinum metal, as catalysts can give significant information about the formation of byproducts especially if their production is due to reactions occurring inside the pores. And finally, to fully commercialize the HYSULF<sup>SM</sup> process, the effect of carbon monoxide, ammonia and other common volatile species present in real refinery streams on the catalyst activity and selectivity have to be studied.

REFERENCES CITED

1. Rall, H. L.; Thompson, C. J.; Coleman, H. J.; and Hopkins, R. L.; Sulfur Compounds in Crude Oil, US Dept. of Interior, Bureau of Mines; Washington, D.C., (1972).
2. Orr, W. L.; and White, C. M. (Editors); Geochemistry of Sulfur in Fossil Fuels, Amer. Chem. Soc., Washington, D.C., PP 2-25 (1990).
3. Satterfield, C. N.; Heterogeneous Catalysis in Practice, McGraw-Hill, New York, pp 235-279 (1980).
4. Othmer, K.; "Encyclopedia of Chemical Technology", 3rd ed., John Wiley and Sons, New York, vol. **17**, pp 125-27 (1983).
5. Gary, J.; and Handwerk, G.; "Petroleum Refining, Technology and Economics", Marcel Dekker, New York (1975).
6. Othmer, K.; "Encyclopedia of Chemical Technology", 3rd ed., vol. **17**, John Wiley and Sons, New York, pp 235-42 (1983).
7. Godish, T.; "Air Quality", 2nd ed., Lewis Publishers, Michigan (1991).
8. Othmer, K.; "Encyclopedia of Chemical Technology", 3rd ed., John Wiley and Sons, New York, vol. **22**, pp 267-82 (1983).
9. Kohl, A.; and Riesenfeld, F.; Gas Purification, 4th ed., Gulf Publishing Company, Houston, pp 251-264, 521-536 (1985).
10. Raymont, M. E.; Hydrocarbon Processing **54**, 139 (1975); and Raymont, M. E., Ph D. Thesis, The University of Calgary, Alta, Canada (1974).
11. Fukuda, K.; Dokiya, M.; Kameyama, T.; and Kotera, Y.; Ind. Eng. Chem. Fundam. **17**(4), 243 (1978).
12. Chivers, T.; Hyne, J.; and Lau, C.; Int. J. Hydrogen

- Energy **5**, 449 (1980).
13. Plummer, M. A.; Hydrocarbon Processing, April (1987).
  14. Krisanti, E.; Mechanism and Kinetics of 2-t-Butylanthraquinone Reduction by Hydrogen Sulfide in Non-aqueous Solvents, PhD Thesis in Chemistry, Colorado School of Mines, (1992).
  15. U. S. EPA ; "National Air Quality and Emission Trends Report", 1976, EPA 450/1-77-002 (1977).
  16. Merck Index, 11th ed., Merck & Co. (1989).
  17. U. S. EPA; "Air Quality Criteria for Particulate Matter and Sulfur Oxides", vol. **II** (1982).
  18. Maddox, R. N.; "Gas and Liquid Sweetening", 2nd ed., John M. Campbell, Norman, pp 1-4 (1977).
  19. Adams, R. W.; Horseman, M. N.; and More, A. I. (Editors); Sulphur **101**, 26 (1972).
  20. Manning, W. P.; Oil and Gas Journal, October 15 (1979).
  21. Hardison, L. C.; Hydrocarbon Processing, April (1985).
  22. Hardison, L. C.; Ramshaw, D.E.; Hydrocarbon Processing, January (1992).
  23. Othmer, K.; "Encyclopedia of Chemical Technology", 3rd ed., vol. **17**, John Wiley and Sons, New York, pp 183-224 (1983).
  24. Othmer, K.; "Encyclopedia of Chemical Technology", 3rd ed., vol. **13**, John Wiley and Sons, New York, pp 16-30 (1983).
  25. Considine, D. M.; "Chemical Process Technology Encyclopedia", McGraw-Hill, New York, p 600 (1975).
  26. Considine, D. M.; "Encyclopedia of Chemistry", Van Nostrand Reinhold, New York, p. 475 (1984).
  27. Jenkins, C. L.; E. I. DuPont De Numerous and Company, U. S. Patent 4,800,075 (Jan. 24, 1989).
  28. Weigert, W.; Delle, H.; and Kaebisch, G.; Chem. Ztg.

- 99(3), 101 (1975).
29. Frerichs, S.; "The Characterization of Pt/Al<sub>2</sub>O<sub>3</sub> and Pt-Re/Al<sub>2</sub>O<sub>3</sub> Reforming Catalysts and their Evaluation Using a Model Naphtha Feedstock", M. S. Thesis, Colorado School of Mines (1984).
  30. Hadsell, K.; "The Effect of Coking and Sulfur Poisoning on Pt/Al<sub>2</sub>O<sub>3</sub> and Pt-Re/Al<sub>2</sub>O<sub>3</sub> Reforming Catalysts Using a Model Naphtha Feedstock", M. S. Thesis, Colorado School of Mines (1985).
  31. Freifeld, M.; "Practical Catalytic Hydrogenation, Techniques and Applications", John Wiley and Sons, New York (1971).
  32. British Patent 1,119,820 (May 6, 1970), (to Oxysynthese).
  33. Riedl, H. J., Ger. Pat. 812,426 (Aug. 30, 1951).
  34. Frosên and Nilsson; "The Chemistry of the Carbonyl Group", (Zabicky, Editor), Vol. 2, Interscience, New York, pp. 157-240 (1970).
  35. Hart; Chemical Rev. **79**, 515 (1979).
  36. Kabisch, G.; and Wittmann, H.; US Patent 3,488,150 (Jan. 6, 1970).
  37. Lait, R.; and Lefevre, C.; British Patent 776, 991 (June 12, 1957).
  38. Makar, K. M.; US Patent 4,061,598 (Dec. 6, 1977).
  39. Linstead, R. P.; Doering, W. E.; Davis, S. B.; and Levine, P.; J. Amer. Chem. Soc. **64**, 185 (1942).
  40. Heyns, K.; and Paulsen, H.; Angew. Chem. **69**, 600 (1957).
  41. Rylander, P. N.; Organic Synthesis with Noble Metal Catalysts, Academic Press, New York, pp 1-59 (1973).
  42. Sheikh, M. Y.; Eadon, G., Tetrahedron Lett. **4**, 257-60 (1972).
  43. Tsai, M-C; Friend, C. M.; and Muetteries, E. L.; J. Amer. Chem. Soc. **104**, 2539 (1982).

44. Fu, P.; and Harvey, R.; Chem. Rev. **78**, 317 (1978).
45. March, J.; Advanced Organic Chemistry, 3rd ed., John Wiley and Sons, New York, pp 1048-1120 (1985).
46. Rylander, P. N.; "Hydrogenation Methods", Academic Press, New York, pp 66-77 (1985).
47. Nishimura, S.; Murai, M.; and Shiota, M.; Chem. Lett., 1239 (1980).
48. Sungbom, C.; and TanaKa, K.; Bull. Chem. Soc. Jpn. **55**, 2275 (1982).
49. Adams, R.; Miyano, S.; and Fles, D.; J. Amer. Chem. Soc. **82**, 1466 (1960).
50. Adams, R.; Miyano, S.; and Nair, M.; J. Amer. Chem. Soc. **32**, 3323 (1961).
51. Nair, M.; and Adams, R.; J. Org. Chem. **26**, 3059 (1961).
52. Rylander, P. N.; and Steele, D. R.; Tetrahedron Lett., 1579 (1969)
53. Dart, M.; and Henbest, H.; J. Chem. Soc., 3563 (1960).
54. Sinfelt, J.; Carter, J.; and Yates Jr., D.; J. Catalysis **24**, 283 (1972).
55. Sinfelt, J.; Acc. Chem. Res. **10**, 15 (1977).
56. Sinfelt, J.; Via, G.; and Lytle, F.; J. Chem. Phys. **76**, 2779 (1982).
57. Hartung, W. H.; and Siminiff, R.; Org. Reactions **7**, 263 (1953).
58. Matsumoto, T.; Endo, Y.; and Okimoto, M.; Bull. Chem. Soc. Jpn. **56**, 2018 (1983).
59. Logsdon, B.; "Development and Characterization of Methanol Decomposition Catalysts" Ph. D. Thesis in Chemistry, Colorado School of Mines, (1989).
60. Cowley, S. W.; and Gebhard, S.; "The Catalytic Conversion of Methanol into Syngas for Use as an

- Automotive Fuel", Colorado School of Mines Quarterly **7** (3), 41 (1983).
61. Wickham, D.; Logsdon, B.; Butler, C.; and Cowley, S.; J. Catalysis **128**, 198 (1991).
  62. Miller, K.; and Wu, J.; J. Catalysis **27**, 60 (1972).
  63. McArthur, D.; Bliss, H.; and Butt, J.; J. Catalysis **28**, 183 (1973).
  64. Brunauer, S.; Emmett, P.; and Teller, E.; J. Amer. Chem. Soc. **60**, 309 (1938).
  65. ASTM, D 1993-91.
  66. Satterfield, C. N.; Heterogeneous Catalysis in Industrial Practice, 2nd ed., McGraw-Hill, New York, pp 134-139 (1991).
  67. Rylander, P. N.; Catalytic Hydrogenation Over Platinum Metals, Academic Press, New York (1967).
  68. Rylander, P. N.; "Catalytic Hydrogenation in Organic Syntheses", Academic Press, New York (1979).
  69. Hudlicky, M.; Reductions in Organic Chemistry, Ellis Horwood Ltd., Chichester (1984).
  70. Gates, B.; Katzer, J.; and Schuit, G., "Chemistry of Catalytic Processes", McGraw-Hill, New York, pp 237-43 (1979).
  71. Imelik, B; Naccache, C.; Coudurier, G; Paraliaud, P.; Meriaudeau, P.; Gallezot, P.; Martin, G.; and Vedrine, J. (Editors), "Studies in Surface Science and Catalysis, No. 11, Metal-Support and Metal-Additive Effects in Catalysis", Elsevier Scientific, Amsterdam (1982).
  72. Dowden, D.; and Kemball, C., "Catalysis, vol. 2, Specialist Periodical Reports", The Chem. Soc. London, pp. 8-11 (1978).
  73. Othmer, K.; "Encyclopedia of Chemical Technology", 3rd ed., vol. **5**, John Wiley and Sons, New York, p 35 (1983).

74. Rylander, P. N.; Hydrogenation Methods, Academic Press, New York (1985).
75. Rylander, P.; and Koch Jr., J., U. S. Patent 3,177,258 (Apr. 1965).
76. Anderson, R. (Editor); "Experimental Methods in Catalytic Research", Academic Press, New York (1968).
77. Dilke, M.; Eley, D.; and Maxted, E.; Nature **161**, 804 (1948).
78. Klug, H.; "X-ray Diffraction Procedures", John Wiley and Sons, New York (1954).
79. Stachurski, J., and Frackiewicz, A.; J. of the Less Common Metals **108**, 249 (1985).